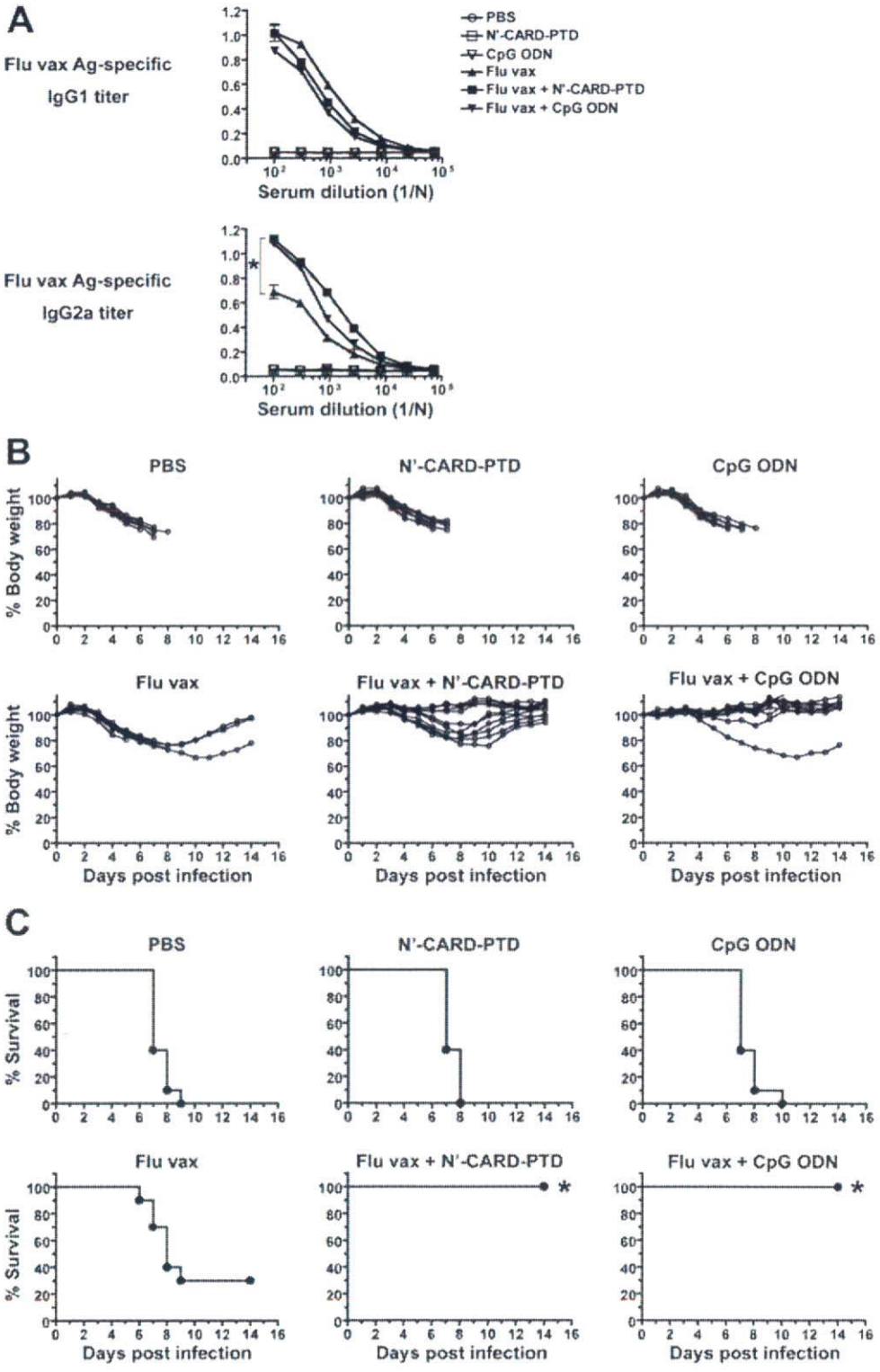

FIGURE 5. Coadministration of N′-CARD-PTD enhances Ag-specific IgG2a production and superior protection against lethal influenza infection. *A–C*, Eight-week-old female BALB/c mice ($n = 10$) were immunized s.c. with flu vax (0.7 μg), N′-CARD-PTD (5 μg), CpG ODN (5 μg), flu vax (0.7 μg) plus N′-CARD-PTD (5 μg), or flu vax (0.7 μg) plus CpG ODN (5 μg) at 0 and 10 days. *A*, Anti-flu vax Ab titer was examined 10 days after the final immunization. *B* and *C*, Ten days after the final immunization, mice were challenged with 8 LD_{50} doses of influenza A/P/R8 (H1N1). The body-weight changes (*B*) and the mortality (*C*) were monitored for the next 14 days. Data represent one of two independent experiments with similar results. *, $p < 0.05$.

with N′-CARD-PTD compared with those stimulated LPS (Fig. 4*B*). These results suggest that N′-CARD-PTD activates a distinct innate immune signaling pathway(s) from those engaged by LPS. In fact, LPS induced phosphorylation of MAPK such as JNK, p38, and ERK within 3 h, while N′-CARD-PTD had little effects on activation of these kinases except for ERK at 3 and 6 h (Fig. 4*B*). We also examined whether N′-CARD-PTD activates bone marrow-derived dendritic cells (BM-DCs). As a control, CpG ODN activated BM-DCs induced in vitro by Flt3L (FL-DCs) but not BM-DCs induced in vitro by GM-CSF (GM-DCs) to produce type I IFNs. N′-CARD-PTD, by contrast, activated both GM-DCs and FL-DCs to produce type I IFNs (Fig. 4*C*). We also observed that N′-CARD-PTD weakly but significantly up-regulated cell surface expression of MHC class I, class II, CD40, and CD86 on both GM-DCs and FL-DCs (data not shown). Up-regulation of such cell surface molecules was dependent on type I IFN production but independent on myeloid differentiation factor 88 (MyD88) nor Toll-IL-1R domain-containing adaptor-inducing IFN-β (TRIF) (data not shown).

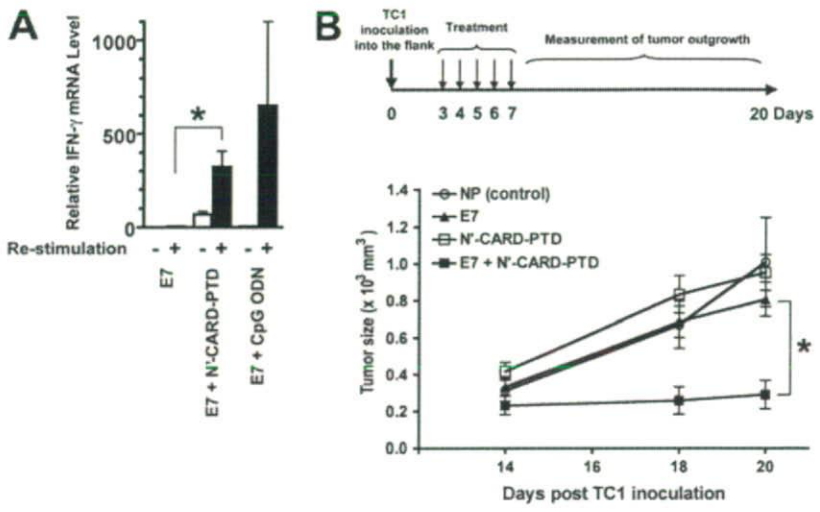

FIGURE 6. Coadministration of N′-CARD-PTD plus tumor-associated Ag E7 confers superior protection against tumor outgrowth. *A*, Eight-week-old female BALB/c mice ($n = 5$) were immunized subcutaneously with E7 peptide (3 μg), E7 peptide (3 μg) plus N′-CARD-PTD (5 μg), or E7 peptide (3 μg) plus CpG ODN (5 μg) at 2 and 4 wk. Splenocytes were prepared from each individual mouse and restimulated in vitro with control NP (−) or E7 peptide (±). The relative expression levels of IFN-γ mRNA were measured by real-time PCR and normalized to 18S rRNA levels. *B*, Eight-week-old C57BL/6 mice ($n = 10$) were inoculated subcutaneously with 1×10^5 TC-1 cells/mouse at 0 days and then immunized with control NP peptide (3 μg), E7 (3 μg), N′-CARD-PTD (5 μg), or E7 (3 μg) plus N′-CARD-PTD (5 μg) at 3, 4, 5, 6, and 7 days. Tumor sizes were measured at 14, 18, and 20 days. Data represent one of two independent experiments with similar results. *, $p < 0.01$.

N′-CARD-PTD augments Ag-specific acquired immune responses to protect against influenza virus infection and tumor outgrowth in vivo

To examine the in vivo effects of N′-CARD-PTD on innate and acquired immune responses, we used a mouse model of influenza virus infection and of tumor transplantation. Influenza split-product vaccine (flu vax) was used to evaluate the adjuvanticity of N′-CARD-PTD. Flu vax was prepared at The Research Foundation for Microbial Diseases of Osaka University from the purified influenza virus A/New Caledonia/20/99 strain treated sequentially with ether and formalin. As shown in Fig. 5*A*, s.c. administration of flu vax plus N′-CARD-PTD or CpG ODN induced significant levels of specific IgG1 production that were comparable to that of flu vax alone. Administration of flu vax plus N′-CARD-PTD or CpG ODN, by contrast, resulted in significantly higher levels of specific IgG2a production compared with that of flu vax alone, suggesting that N′-CARD-PTD and CpG ODN have the ability to modulate Th1-deviated immune responses. In accordance with such adjuvant effects, immunization with flu vax plus N′-CARD-PTD conferred superior protection against a lethal influenza challenge relative to that with flu vax alone (Fig. 5, *B* and *C*).

We next examined whether N′-CARD-PTD has an ability to enhance Ag-specific cellular immune responses. Immunization with MHC class I-restricted HPV E7 peptide (E7) alone induced minimal levels of E7-specific IFN-γ production from splenocytes (Fig. 6*A*). Treatment with E7 plus N′-CARD-PTD or CpG ODN induced higher levels of E7-specific IFN-γ production, suggesting that N′-CARD-PTD has an adjuvant effect on cell-mediated immune responses (Fig. 6*A*). Thus, mice were s.c. transplanted with TC-1 cells expressing E7 as a model tumor Ag, and then immunized with E7 in the presence or absence of N′-CARD-PTD, as shown in Fig. 6*B*. The outgrowth of TC-1 tumors in mice treated with either N′-CARD-PTD or E7 alone was comparable to that in mice treated with control NP peptide. In accordance with E7-specific IFN-γ production from splenocytes, the sizes of established tumors in mice treated with E7 plus N′-CARD-PTD were significantly smaller compared with those in mice treated with E7 alone or with N′-CARD-PTD alone (Fig. 6*B*). These in vivo results, taken together, indicate that N′-CARD-PTD, an activator of NDH-mediated innate immune responses, acts as a vaccine adjuvant, thereby enhancing protective immune responses against pathogens or tumors.

Discussion

This study provides the first evidence that the N′-CARD-PTD polypeptide directly enters the nucleus and triggers the innate immune signaling pathway leading to type I IFN production through NDH. NDH is a member of the DEXH (Asp-Glu-X-His) family of helicases and is highly conserved in higher eukaryotes, from *Drosophila* to mammals. Previous studies have shown that NDH interacts with molecules of the transcription machinery, such as the RNA polymerase II complex (28), cAMP-response element-binding protein (28), and NF-κB p65 (29), thereby regulating the transcription of responsive genes. NDH also acts together with the RNA editing enzyme to coordinate the editing and splicing of numerous cellular and viral RNAs (30, 31). Knockout of the *Ndh* gene led to early embryonic lethality (<E10.5) due to a high frequency of apoptosis in embryonic ectodermal cells during gastrulation (32). In addition to these properties of gene regulation and cellular homeostasis, our results suggest that NDH has a distinct property of mediating innate immune signaling upstream of TBK1. Recently, it was shown that a DEAD (Asp-Glu-Ala-Asp) box helicase, DDX3X, is a kinase substrate of TBK1 and acts as a critical component of TBK1-dependent innate immune signaling, particularly in the type I IFN production pathway (33).

MAPK activation plays a significant role in LPS- or CpG DNA-mediated signaling (Fig. 4*C* and Ref. 34), however, the signaling pathway induced by N′-CARD-PTD may not involve MAPK. This suggested that, unlike TLR-mediated signaling pathways, activation of MAPK is not crucial for N′-CARD-PTD-mediated type I IFN production. Rather, the action of N′-CARD-PTD resembles the signal activation induced by IFN stimulatory DNA, which was originally reported by Stetson et al. as having a similar action to B-DNA, which is critical in the control of DNA vaccine immunogenicity (5, 35). Because MAPK activation is associated with deleterious effects, ranging from hyperinflammation to cancer (36), the lack of such kinase activation would be an advantage for the repeated clinical application of N′-CARD-PTD. Further study will be needed to elucidate the molecular basis of the NDH-mediated signaling pathway and to determine the value of N′-CARD-PTD for clinical use.

Many TLR ligands and related compounds have been tested as vaccine adjuvants and as anti-allergy and anti-cancer drugs in humans (37). Among these, some clinical trials of TLR9-targeting molecules, including CpG ODN and its conjugated products, have recently been abandoned due to unexpectedly weaker responses in

humans relative to those observed in mice. This result was attributable to a lower frequency of TLR9 expression in human immune cells; expression was found in only a portion of B cells and plasmacytoid DCs that combined made up just 1% of the total immune cell population (38). In contrast, immunostimulatory RNA or B-DNA activates innate immune responses through cytosolic receptors but only when they are introduced into intracellular compartments, i.e., they have almost no effects when they are present outside the cell. Taking such observations into account, N′-CARD-PTD may have the advantage of self-transmigration into the nucleus and of triggering innate immune signaling in the absence of TLRs but in the presence of NDH and TBK1, which are ubiquitously expressed in a wide-variety of cell types.

In conclusion, this study showed concrete evidence that the activation of a distinct NDH-mediated signaling pathway up-regulates innate immune responses and that N′-CARD-PTD is a candidate vaccine adjuvant in future vaccine development. These findings may also provide insights that will be helpful in the design of immunomodulatory agents, such as using constitutively active signaling molecules of the innate immune responses.

Disclosures

The authors have no financial conflict of interest.

References

1. Barr, S. D., J. R. Smiley, and F. D. Bushman. 2008. The interferon response inhibits HIV particle production by induction of TRIM22. *PLoS Pathog.* 4: 1–11.
2. Fodil-Cornu, N., and S. M. Vidal. 2008. Type I interferon response to cytomegalovirus infection: the kick-start. *Cell Host Microbes* 3: 59–61.
3. Bracci, L., E. Proietti, and F. Belardelli. 2007. IFN-α and novel strategies of combination therapy for cancer. *Ann. NY Acad. Sci.* 1112: 256–268.
4. Ferrantini, M., I. Capone, and F. Belardelli. 2007. Interferon-α and cancer: mechanisms of action and new perspectives of clinical use. *Biochimie* 89: 884–893.
5. Ishii, K. J., T. Kawagoe, S. Koyama, K. Matsui, H. Kumar, T. Kawai, S. Uematsu, O. Takeuchi, F. Takeshita, C. Coban, and S. Akira. 2008. TANK-binding kinase-1 delineates innate and adaptive immune responses to DNA vaccines. *Nature* 451: 725–729.
6. Ishii, K. J., C. Coban, H. Kato, K. Takahashi, Y. Torii, F. Takeshita, H. Ludwig, G. Sutter, K. Suzuki, H. Hemmi, et al. 2006. A Toll-like receptor-independent antiviral response induced by double-stranded B-form DNA. *Nat. Immunol.* 7: 40–48.
7. Zhu, J., X. Huang, and Y. Yang. 2007. Innate immune response to adenoviral vectors is mediated by both Toll-like receptor-dependent and -independent pathways. *J. Virol.* 81: 3170–3180.
8. Takeuchi, O., and S. Akira. 2008. MDA5/RIG-I and virus recognition. *Curr. Opin. Immunol.* 20: 17–22.
9. Kawai, T., and S. Akira. 2007. Antiviral signaling through pattern recognition receptors. *J. Biochem.* 141: 137–145.
10. Yoshida, H., Y. Okabe, K. Kawane, H. Fukuyama, and S. Nagata. 2005. Lethal anemia caused by interferon-β produced in mouse embryos carrying undigested DNA. *Nat. Immunol.* 6: 49–56.
11. Kawane, K., M. Ohtani, K. Miwa, T. Kizawa, Y. Kanbara, Y. Yoshioka, H. Yoshikawa, and S. Nagata. 2006. Chronic polyarthritis caused by mammalian DNA that escapes from degradation in macrophages. *Nature* 443: 998–1002.
12. Kato, H., O. Takeuchi, S. Sato, M. Yoneyama, M. Yamamoto, K. Matsui, S. Uematsu, A. Jung, T. Kawai, K. J. Ishii, et al. 2006. Differential roles of MDA5 and RIG-I helicases in the recognition of RNA viruses. *Nature* 441: 101–105.
13. Cheng, G., J. Zhong, J. Chung, and F. V. Chisari. 2007. Double-stranded DNA and double-stranded RNA induce a common antiviral signaling pathway in human cells. *Proc. Natl. Acad. Sci. USA* 104: 9035–9040.
14. Takahasi, K., M. Yoneyama, T. Nishihori, R. Hirai, H. Kumeta, R. Narita, M. Gale, Jr., F. Inagaki, and T. Fujita. 2008. Nonself RNA-sensing mechanism of RIG-I helicase and activation of antiviral immune responses. *Mol. Cell* 29: 428–440.
15. Ishii, K. J., S. Koyama, A. Nakagawa, C. Coban, and S. Akira. 2008. Host innate immune receptors and beyond: making sense of microbial infections. *Cell Host Microbes* 3: 352–363.
16. Potter, J. A., R. E. Randall, and G. L. Taylor. 2008. Crystal structure of human IPS-1/MAVS/VISA/Cardif caspase activation recruitment domain. *BMC Struct. Biol.* 8: 11.
17. Loo, Y. M., D. M. Owen, K. Li, A. K. Erickson, C. L. Johnson, P. M. Fish, D. S. Carney, T. Wang, H. Ishida, M. Yoneyama, et al. 2006. Viral and therapeutic control of IFN-β promoter stimulator 1 during hepatitis C virus infection. *Proc. Natl. Acad. Sci. USA* 103: 6001–6006.
18. Sung, M., G. M. Poon, and J. Gariepy. 2006. The importance of valency in enhancing the import and cell routing potential of protein transduction domain-containing molecules. *Biochim. Biophys. Acta* 1758: 355–363.
19. Davenport, F. M., A. V. Hennessy, F. M. Brandon, R. G. Webster, C. D. Barrett, Jr., and G. O. Lease. 1964. Comparisons of serologic and febrile responses in humans to vaccination with influenza a viruses or their hemagglutinins. *J. Lab. Clin. Med.* 63: 5–13.
20. Tanimoto, T., R. Nakatsu, I. Fuke, T. Ishikawa, M. Ishibashi, K. Yamanishi, M. Takahashi, and S. Tamura. 2005. Estimation of the neuraminidase content of influenza viruses and split-product vaccines by immunochromatography. *Vaccine* 23: 4598–4609.
21. Kawai, T., K. Takahashi, S. Sato, C. Coban, H. Kumar, H. Kato, K. J. Ishii, O. Takeuchi, and S. Akira. 2005. IPS-1, an adaptor triggering RIG-I- and Mda5-mediated type I interferon induction. *Nat. Immunol.* 6: 981–988.
22. Jounai, N., F. Takeshita, K. Kobiyama, A. Sawano, A. Miyawaki, K. Q. Xin, K. J. Ishii, T. Kawai, S. Akira, K. Suzuki, and K. Okuda. 2007. The Atg5 Atg12 conjugate associates with innate antiviral immune responses. *Proc. Natl. Acad. Sci. USA* 104: 14050–14055.
23. Takeshita, F., K. Suzuki, S. Sasaki, N. Ishii, D. M. Klinman, and K. J. Ishii. 2004. Transcriptional regulation of the human TLR9 gene. *J. Immunol.* 173: 2552–2561.
24. Takeshita, F., K. J. Ishii, K. Kobiyama, Y. Kojima, C. Coban, S. Sasaki, N. Ishii, D. M. Klinman, K. Okuda, S. Akira, and K. Suzuki. 2005. TRAF4 acts as a silencer in TLR-mediated signaling through the association with TRAF6 and TRIF. *Eur. J. Immunol.* 35: 2477–2485.
25. Takeshita, F., T. Tanaka, T. Matsuda, M. Tozuka, K. Kobiyama, S. Saha, K. Matsui, K. J. Ishii, C. Coban, S. Akira, et al. 2006. Toll-like receptor adaptor molecules enhance DNA-raised adaptive immune responses against influenza and tumors through activation of innate immunity. *J. Virol.* 80: 6218–6224.
26. Seth, R. B., L. Sun, C. K. Ea, and Z. J. Chen. 2005. Identification and characterization of MAVS, a mitochondrial antiviral signaling protein that activates NF-κB and IRF 3. *Cell* 122: 669–682.
27. Fitzgerald, K. A., S. M. McWhirter, K. L. Faia, D. C. Rowe, E. Latz, D. T. Golenbock, A. J. Coyle, S. M. Liao, and T. Maniatis. 2003. IKKε and TBK1 are essential components of the IRF3 signaling pathway. *Nat. Immunol.* 4: 491–496.
28. Nakajima, T., C. Uchida, S. F. Anderson, C. G. Lee, J. Hurwitz, J. D. Parvin, and M. Montminy. 1997. RNA helicase A mediates association of CBP with RNA polymerase II. *Cell* 90: 1107–1112.
29. Tetsuka, T., H. Uranishi, T. Sanda, K. Asamitsu, J. P. Yang, F. Wong-Staal, and T. Okamoto. 2004. RNA helicase A interacts with nuclear factor κB p65 and functions as a transcriptional coactivator. *Eur. J. Biochem.* 271: 3741–3751.
30. Bratt, E., and M. Ohman. 2003. Coordination of editing and splicing of glutamate receptor pre-mRNA. *RNA* 9: 309–318.
31. Maas, S., A. Rich, and K. Nishikura. 2003. A-to-I RNA editing: recent news and residual mysteries. *J. Biol. Chem.* 278: 1391–1394.
32. Lee, C. G., V. da Costa Soares, C. Newberger, K. Manova, E. Lacy, and J. Hurwitz. 1998. RNA helicase A is essential for normal gastrulation. *Proc. Natl. Acad. Sci. USA* 95: 13709–13713.
33. Soulat, D., T. Burckstummer, S. Westermayer, A. Goncalves, A. Bauch, A. Stefanovic, O. Hantschel, K. L. Bennett, T. Decker, and G. Superti-Furga. 2008. The DEAD-box helicase DDX3X is a critical component of the TANK-binding kinase 1-dependent innate immune response. *EMBO J.* 27: 2135–2146.
34. Hacker, H., H. Mischak, G. Hacker, S. Eser, N. Prenzel, A. Ullrich, and H. Wagner. 1999. Cell type-specific activation of mitogen-activated protein kinases by CpG-DNA controls interleukin-12 release from antigen-presenting cells. *EMBO J.* 18: 6973–6982.
35. Stetson, D. B., and R. Medzhitov. 2006. Recognition of cytosolic DNA activates an IRF3-dependent innate immune response. *Immunity* 24: 93–103.
36. Salh, B. 2007. c-Jun N-terminal kinases as potential therapeutic targets. *Expert Opin. Ther. Targets.* 11: 1339–1353.
37. Kanzler, H., F. J. Barrat, E. M. Hessel, and R. L. Coffman. 2007. Therapeutic targeting of innate immunity with Toll-like receptor agonists and antagonists. *Nat. Med.* 13: 552–559.
38. Schmidt, C. 2007. Clinical setbacks for Toll-like receptor 9 agonists in cancer. *Nat. Biotechnol.* 25: 825–826.

Published Ahead of Print on March 16, 2009 as 10.1200/JCO.2008.19.9745
The latest version is at http://jco.ascopubs.org/cgi/doi/10.1200/JCO.2008.19.9745

JOURNAL OF CLINICAL ONCOLOGY ORIGINAL REPORT

Identification of a Predictive Biomarker for Hematologic Toxicities of Gemcitabine

Junichi Matsubara, Masaya Ono, Ayako Negishi, Hideki Ueno, Takuji Okusaka, Junji Furuse, Koh Furuta, Emiko Sugiyama, Yoshiro Saito, Nahoko Kaniwa, Junichi Sawada, Kazufumi Honda, Tomohiro Sakuma, Tsutomu Chiba, Nagahiro Saijo, Setsuo Hirohashi, and Tesshi Yamada

From the Chemotherapy Division, National Cancer Center Research Institute; Hepatobiliary and Pancreatic Oncology Division and Clinical Laboratory Division, National Cancer Center Hospital; Project Team for Pharmacogenetics, National Institute of Health Sciences; BioBusiness Group, Mitsui Knowledge Industry, Tokyo; Hepatobiliary and Pancreatic Oncology Division, National Cancer Center Hospital East, Kashiwa; and Department of Gastroenterology and Hepatology, Kyoto University Graduate School of Medicine, Kyoto, Japan.

Submitted September 3, 2008; accepted December 1, 2008; published online ahead of print at www.jco.org on March 16, 2009.

Supported by the Program for Promotion of Fundamental Studies in Health Sciences conducted by the National Institute of Biomedical Innovation of Japan, the Third-Term Comprehensive Control Research for Cancer conducted by the Ministry of Health and Labor of Japan, and generous grants from the Naito Foundation, the Princess Takamatsu Cancer Research Fund, and the Foundation for the Promotion of Cancer Research. These sponsors had no role in the design of the study, the collection of the data, the analysis and interpretation of the data, the decision to submit the article for publication, or the writing of the article.

Authors' disclosures of potential conflicts of interest and author contributions are found at the end of this article.

Corresponding author: Tesshi Yamada, MD, PhD, Chemotherapy Division, National Cancer Center Research Institute, 5-1-1 Tsukiji, Chuo-ku, Tokyo 104-0045, Japan; e-mail: tyamada@ncc.go.jp.

© 2009 by American Society of Clinical Oncology

0732-183X/09/2799-1/$20.00

DOI: 10.1200/JCO.2008.19.9745

ABSTRACT

Purpose
Gemcitabine monotherapy is the current standard for patients with advanced pancreatic cancer, but the occurrence of severe neutropenia and thrombocytopenia can sometimes be life threatening. This study aimed to discover a new diagnostic method for predicting the hematologic toxicities of gemcitabine.

Patients and Methods
Using quantitative mass spectrometry (MS), we compared the baseline plasma proteomes of 25 patients who had developed severe hematologic adverse events (grade 3 to 4 neutropenia and/or grade 2 to 4 thrombocytopenia) within the first two cycles of gemcitabine with those of 22 patients who had not (grade 0).

Results
We identified 757 peptide peaks whose intensities were significantly different ($P < .001$, Welch t test) among a total of 60,888. The MS peak with the highest statistical significance ($P = .0000282$) was revealed to be derived from haptoglobin by tandem MS. A scoring system (nomogram) based on the values of haptoglobin, haptoglobin phenotype, neutrophil count, platelet count, and body-surface area was constructed to estimate the risk of hematologic adverse events (grade 3 to 4 neutropenia and/or grade 2 to 4 thrombocytopenia) with an area under curve value of 0.782 in a cohort of 166 patients with pancreatic cancer. Predictive ability of the system was confirmed in two independent validation cohorts consisting of 87 and 52 patients with area under the curve values of 0.655 and 0.747, respectively.

Conclusion
Although the precise mechanism responsible for the correlation of haptoglobin with the future onset of hematologic toxicities remains to be clarified, our prediction model seems to have high practical utility for tailoring the treatment of patients receiving gemcitabine.

J Clin Oncol 27. © 2009 by American Society of Clinical Oncology

INTRODUCTION

Pancreatic adenocarcinoma is one of the most aggressive and lethal cancers.[1] It is the fifth leading cause of cancer-related mortality in Japan and the fourth leading cause in the United States, accounting for an estimated more than 23,000 annual deaths in Japan and more than 33,000 deaths in the United States.[2,3] The median survival time of patients with advanced pancreatic cancer had remained at only 3 to 4 months until the introduction of the nucleoside anticancer drug gemcitabine (2′,2′-difluorodeoxycytidine). Gemcitabine monotherapy extended the overall survival of pancreatic cancer patients up to 6 months, along with significant clinical benefits such as pain relief and improvement of performance status,[4-6] and is now accepted as a standard first-line treatment for unresectable advanced pancreatic cancer.[7] However, hematologic toxicity is the dose-limiting factor of gemcitabine therapy.[8] Although severe nonhematologic toxicity is infrequent,[4-6] 20% to 30% of patients receiving gemcitabine experience grade 3 to 4 neutropenia (National Cancer Institute [NCI] Common Toxicity Criteria, version 2.0), and approximately 10% experience grade 3 to 4 thrombocytopenia.[5,6,9,10] These levels of severe hematologic adverse events (AEs) can be potentially life threatening.

Several attempts have been made to predict the occurrence of AE associated with chemotherapy. Old age, poor performance status, and reduced initial blood cell counts have been reported to be the risk factors of hematotoxicities.[11,12] To further improve prediction accuracy, combinations of these

Information downloaded from jco.ascopubs.org and provided by Kokuritsu Gan Center on March 24, 2009 from .
Copyright © 2009 by the American Society of Clinical Oncology. All rights reserved.
Copyright 2009 by American Society of Clinical Oncology

risk factors have also been proposed,[11-14] but no reliable predictor has been established for gemcitabine-induced hematologic AEs. We previously identified a significant correlation of a nonsynonymous single nucleotide polymorphism of the cytidine deaminase (*CDA*) gene with altered pharmacokinetics of gemcitabine, but its prediction accuracy for hematologic AE was not satisfactory.[15,16]

Recent advanced proteomic technologies have been increasingly applied to studies of clinical samples[17] to identify biomarkers that could facilitate the tailoring of cancer treatments. Protein expression is not always correlated with mRNA expression,[18] and it is anticipated that alterations in the protein content of clinical samples more directly reflect the biologic and pathologic status of patients. Matrix-assisted laser desorption/ionization mass spectrometry (MS) is becoming a method of choice for profiling of clinical samples as a result of its high sensitivity and throughput. In fact, previous studies have successfully identified biomarkers that could predict the outcome of cancer patients and the efficacy of molecular-targeting drugs.[19,20] However, only low molecular weight proteins can be analyzed by matrix-assisted laser desorption/ionization MS, and thus, a method allowing more comprehensive protein profiling is desirable.

Shotgun proteomics is an emerging concept in which whole proteins are enzymatically digested into a large array of small peptide fragments having uniform physical and chemical characteristics and then analyzed directly by MS. We previously developed a new platform, namely two-dimensional image converted analysis of liquid chromatography and mass spectrometry (2DICAL), to give a quantitative dimension to shotgun proteomics.[21] To identify new biomarkers that might be useful for prediction of gemcitabine-induced neutropenia and thrombocytopenia in patients with pancreatic cancer, we compared the plasma protein profiles of two extreme populations of patients who had shown different responses to the same gemcitabine treatment by 2DICAL. Here we report the identification of plasma/serum haptoglobin as a biomarker of hematologic toxicities associated with gemcitabine treatment.

PATIENTS AND METHODS

Patients

Plasma or serum samples were collected from three cohorts (modeling [M0], validation-1 [V1], and validation-2 [V2] cohorts) totaling 305 patients. All the patients had locally advanced or metastatic (stage IVA or IVB),[22] histologically or cytologically proven pancreatic ductal adenocarcinoma and received at least two cycles of gemcitabine monotherapy (1,000 mg/m^2 intravenously over 30 minutes on days 1, 8, and 15 of a 28-day cycle). Demographic and laboratory data for the patients before administration of gemcitabine are listed in Appendix Tables A1 to A3 (online only). The severity of early hematologic AEs that appeared within the first two cycles of the gemcitabine treatment was graded according to NCI Common Terminology Criteria for Adverse Events (CTCAE; version 3.0).

Cohort M0 comprised 166 patients who had been enrolled onto our previous study at the National Cancer Center (NCC) Hospital (Tokyo, Japan) and Hospital East (Kashiwa, Japan) between September 2002 and July 2004.[15,16] Cohort V1 comprised 87 patients who had been treated consecutively at the NCC Hospital between August 2005 and June 2007, and cohort V2 comprised 52 patients treated at the NCC Hospital consecutively between August 2004 and July 2005.

Sample Preparation

Blood was drawn before the administration of gemcitabine. Plasma (cohorts M0 and V1) or serum (cohort V2) was separated by centrifugation at 4°C and frozen at −70°C (cohort M0) or −20°C (cohorts V1 and V2) until analysis. Macroscopically hemolyzed samples were excluded from the current analysis. The protocol of this retrospective study was reviewed and approved by the institutional ethics committee boards of the NCC (Tokyo, Japan) and the National Institute of Health Sciences (Tokyo, Japan).

Liquid Chromatography/MS

Samples were passed through an IgY-12 High Capacity Spin Column (Beckman Coulter, Fullerton, CA) in accordance with the manufacturer's instructions to reduce the amounts of the 12 most abundant plasma proteins. The flow-through portion was digested with sequencing-grade modified trypsin (Promega, Madison, WI) and analyzed in triplicate using a nano-flow high-performance liquid chromatograph (NanoFrontier nLC; Hitachi High-Technologies, Tokyo, Japan) connected to an electrospray ionization quadrupole time-of-flight (ESI-Q-TOF) mass spectrometer (Q-Tof Ultima; Waters, Milford, MC).

MS peaks were detected, normalized, and quantified using the in-house 2DICAL software package, as described previously.[21] A serial identification (ID) number was applied to each of the MS peaks detected (1 to 60,888). The stability of liquid chromatography/MS was monitored by calculating the correlation coefficient of every triplicate measurement. The mean correlation coefficient (±standard deviation) of the entire 60,888 peaks of the 47 triplicate runs was as high as 0.978 (±0.017).

Tandem MS

Peak lists were generated using the Mass Navigator software package (version 1.2; Mitsui Knowledge Industry, Tokyo, Japan) and searched against the SwissProt database (downloaded from http://www.expasy.ch/sprot/sprot-top.html on October 18, 2007) using the Mascot software package (version 2.2.1; Matrix Science, London, United Kingdom). The score threshold was set to $P < .05$ based on the size of the database used in the search.

Western Blot Analysis

Primary antibodies used were rabbit polyclonal antibody against human haptoglobin (Dako, Glostrup, Denmark) and mouse monoclonal antibody against human complement C3b-α (Progen, Heidelberg, Germany). Ten microliters of partitioned sample were separated by sodium dodecyl sulfate–polyacrylamide gel electrophoresis (SDS-PAGE) and electroblotted onto a polyvinylidene difluoride membrane. The membrane was then incubated with the primary antibody and subsequently with relevant horseradish peroxidase–conjugated antirabbit or antimouse immunoglobulin G as described previously.[23,24] Blots were developed using an enhanced chemiluminescence (ECL) detection system (GE Healthcare, Buckinghamshire, United Kingdom).

Quantification and Subtyping of Haptoglobin

The concentration of plasma or serum haptoglobin was measured using an automated immunonephelometry BN-II system (Siemens Healthcare Diagnostics, Tokyo, Japan). The phenotype of haptoglobin α-chain was determined by nondenaturing (native) SDS-PAGE.[25]

Categorization of Hematologic Toxicities

Overall severity of hematologic toxicities after gemcitabine treatment was classified into categories I to IV based on the worst CTCAE grades of neutropenia and thrombocytopenia (Appendix Fig A1, online only), as follows: category I, grade 0 to 1 neutropenia and grade 0 thrombocytopenia; category II, grade 2 neutropenia or grade 1 thrombocytopenia; category III, grade 3 neutropenia or grade 2 thrombocytopenia; and category IV, grade 4 neutropenia or grade 3 to 4 thrombocytopenia.

Statistical Analysis

Statistical significance of intergroup differences was assessed using the Welch t test, χ^2 test, Wilcoxon test, or Kruskal-Wallis test, as appropriate. Multivariate regression analysis was performed using ordinal logistic regression modeling. Factors included in the prediction model were selected with a forward stepwise selection procedure using Akaike's Information Criterion (AIC). To correct biased sample sizes of categories, each observation was weighted according to the sample size of its category in the fitting process. The significance of differences between models with and without haptoglobin was assessed with the likelihood ratio test. Statistical analyses were performed using

 © 2009 by American Society of Clinical Oncology

Information downloaded from jco.ascopubs.org and provided by Kokuritsu Gan Center on March 24, 2009 from .
Copyright © 2009 by the American Society of Clinical Oncology. All rights reserved.

an open-source statistical language R (version 2.7.0; http://www.r-project.org/) with the optional module design package.

RESULTS

Plasma Proteins Associated With Hematologic AEs

To identify a biomarker that can predict the occurrence of hematologic AEs associated with gemcitabine treatment, we compared the baseline plasma proteome between 25 patients who developed severe AEs (grade 3 to 4 neutropenia and/or grade 2 to 4 thrombocytopenia) and 22 patients who did not (grade 0) using 2DICAL. These levels of hematologic AEs have been used as criteria for dose reduction or postponement of gemcitabine-based treatments.[26-28] There was no significant difference in age, sex, Eastern Cooperative Oncology Group performance status, routine biochemical laboratory data, or pharmacokinetics of gemcitabine[15] (Table 1 and data not shown) between the two extreme groups of patients who were selected from cohort M0, but the patients who experienced severe AEs had significantly lower baseline peripheral-blood leukocyte, neutrophil, and platelet counts than patients without AEs (Table 1).

Among a total of 60,888 independent MS peaks detected within the range of 250 to 1,600 m/z and within the time range 20 to 70 minutes, we found that the mean intensity of triplicates differed significantly in 757 peaks ($P < .001$, Welch t test). Figure 1A is a representative two-dimensional view of all the MS peaks displayed with m/z along the x-axis and the retention time of LC along the y-axis. The 757 MS peaks whose expression differed significantly between patients with severe AEs and patients without AEs are highlighted in red.

One hundred fifteen MS/MS spectra acquired from 200 peaks with the smallest P values were matched to 41 proteins in the database (Mascot score of > 15; Appendix Tables A4 and A5, online only). Notably, MS peaks including one that was decreased in patients with severe AEs with the highest statistical significance ($P = .0000282$; Fig 1B) most recurrently (six times) matched the amino acid sequences of the haptoglobin (*HP*) gene product (Appendix Fig A2, online only). Figure 2A shows the distribution of two representative haptoglobin-derived MS peaks (ID 2062 [at 491 m/z and 44.5 minutes] and ID 5681 [at 602 m/z and 47 minutes]) in patients with severe AEs and without AEs. The differential expression and identification of haptoglobin were confirmed by denaturing SDS-PAGE and immunoblotting (Fig 2B).

Correlation of Haptoglobin With the Degree of Hematologic Toxicities

The levels of haptoglobin in plasma or serum samples obtained from 305 patients with advanced pancreatic cancer before gemcitabine treatment were measured by immunonephelometry and compared with the occurrence and severity of hematologic AEs. Consistent with 2DICAL analysis, the plasma levels of haptoglobin were significantly lower in the 25 patients with severe AEs than in the 22 patients without AEs ($P = .0002$, Wilcoxon test; Table 1).

The plasma level of haptoglobin showed a significant correlation with the NCI-CTCAE grade of neutropenia ($P = .012$, Kruskal-Wallis test) and hematologic toxicity categories ($P = .001$) in the 166 patients of cohort M0 (Fig 3A and Appendix Table A1). The correlation of haptoglobin levels with the grades of neutropenia and thrombocytopenia as well as the toxicity categories was consistently observed in the

Table 1. Clinical and Laboratory Data of Patients Without AEs and With Severe AEs

Factor	Patients Without AEs (n = 22)	Patients With Severe AEs (n = 25)	P
Haptoglobin, mg/dL			.0002
Mean	286	155	
SD	130	59	
Haptoglobin phenotype, No. of patients			.705*
Hp 2-2	12	14	
Hp 2-1	8	7	
Hp 1-1	2	4	
Sex, No. of patients			.344*
Male	12	17	
Female	10	8	
Age, years			.616
Mean	64	63	
SD	8	8	
ECOG performance status, No. of patients			.862*
0	12	13	
1	10	12	
2	0	0	
Body-surface area, m^2			.733
Mean	1.51	1.53	
SD	0.20	0.18	
Prior therapy, No. of patients			.867*
None	19	22	
Chemoradiotherapy using FU for LAPC	3	3	
Leucocyte, $\times 10^3/\mu L$			.0002
Mean	7.4	4.8	
SD	2.8	1.4	
Absolute neutrophil count, $\times 10^3/\mu L$			.0002
Mean	5.3	3.0	
SD	2.4	1.1	
Platelet, $\times 10^4/\mu L$			< .0001
Mean	28	17	
SD	11	6	
Hemoglobin, g/dL			.806
Mean	12.1	11.9	
SD	1.4	1.4	
Albumin, g/dL			.131
Mean	3.6	3.7	
SD	0.4	0.3	
Creatinine, mg/dL			.931
Mean	0.72	0.70	
SD	0.25	0.17	
AST, U/L			.430
Mean	37	29	
SD	26	13	
ALT, U/L			.624
Mean	43	32	
SD	37	24	
ALP, U/L			.815
Mean	593	459	
SD	591	283	
Pharmacokinetic parameters of gemcitabine			
C_{max}, μg/mL			.594
Mean	24.02	23.21	
SD	7.18	6.68	
AUC, h · μg/mL			.462
Mean	9.95	10.74	
SD	2.36	3.03	

NOTE. Kruskal-Wallis test was applied to assess differences of values.
Abbreviations: AE, adverse event; SD, standard deviation; ECOG, Eastern Cooperative Oncology Group; FU, fluorouracil; LAPC, locally advanced pancreatic cancer; ALP, alkaline phosphatase; C_{max}, peak concentration; AUC, area under the curve.
*Calculated using the χ^2 test.

© 2009 by American Society of Clinical Oncology

Information downloaded from jco.ascopubs.org and provided by Kokuritsu Gan Center on March 24, 2009 from .
Copyright © 2009 by the American Society of Clinical Oncology. All rights reserved.

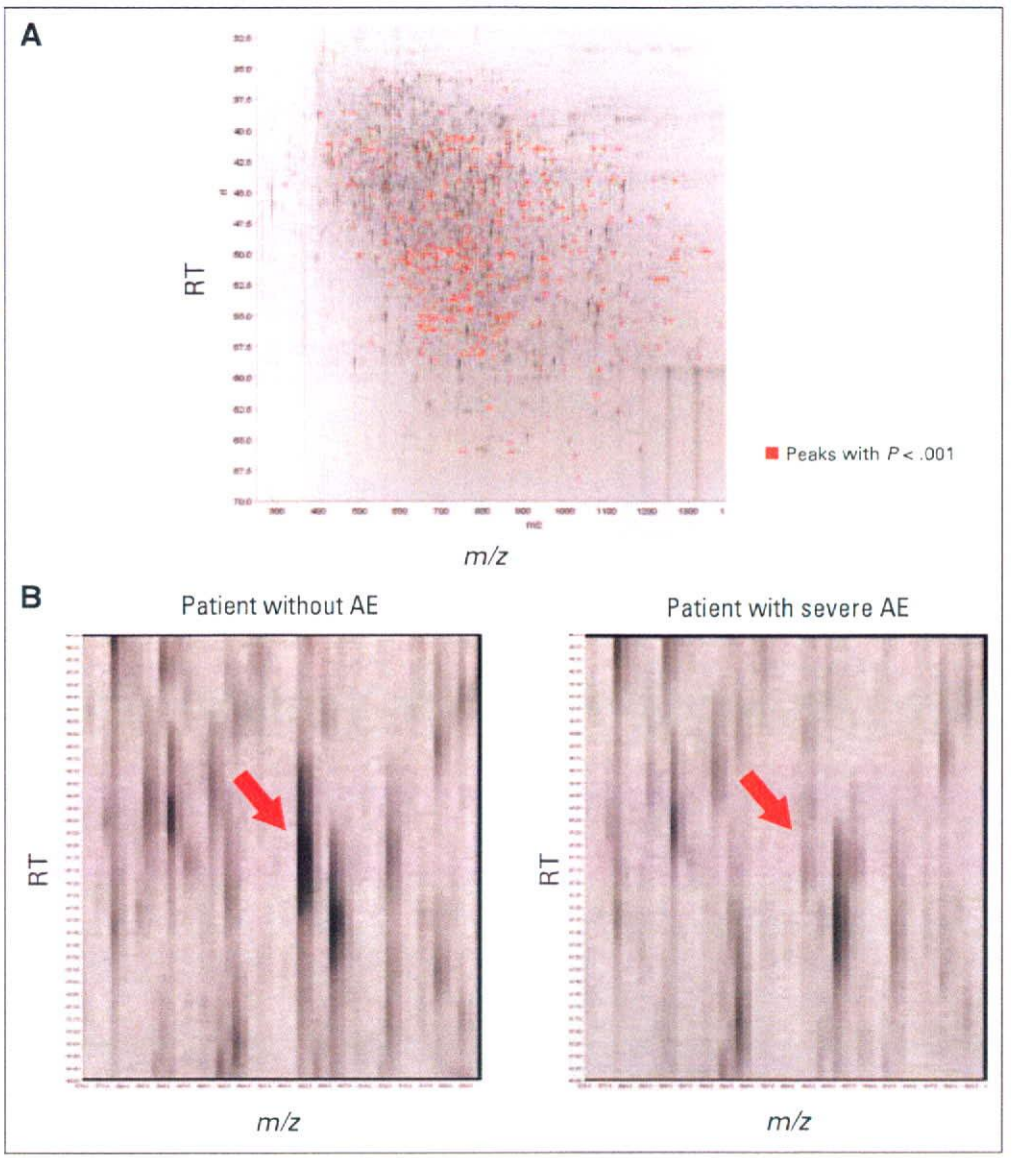

Fig 1. (A) Two-dimensional display of the entire (> 60,000) mass spectrometry (MS) peaks. The 757 MS peaks whose mean intensity differed significantly between patients with severe adverse events (AEs) and patients without AEs ($P < .001$, Welch t test) are highlighted in red. (B) MS peak with the smallest P value ($P = .0000282$; red arrows) in representative patients with severe AEs (right) and without AEs (left). RT, retention time.

two independent validation cohorts V1 (Fig 3B and Appendix Table A2) and V2 (Fig 3C and Appendix Table A3). The correlations between the levels of haptoglobin and the toxicity categories showed the highest statistical significance in all three cohorts (Figs 3A to 3C). The toxicity categories are criteria that we devised to evaluate the clinical severity of overall hematologic toxicities with emphasis on thrombocytopenia (Appendix Fig A1) from a practical viewpoint.[26-28] The management of neutropenia is largely uncomplicated because of the availability of granulocyte colony-stimulating factor.

Haptoglobin Phenotype and Hematologic Toxicities

Haptoglobin is a plasma protein that binds free hemoglobin and inhibits its oxidative activity. The human *HP* gene has two common polymorphic alleles (*H1* and *H2*), yielding individuals with the following three distinct phenotypes in the α-chain of haptoglobin protein: Hp 1-1, Hp 2-1, and Hp 2-2. The *H2* genotype has been reported to be associated with an increased risk of myocardial infarction and juvenile diabetes.[29] Although the frequency of the three phenotypes did not differ significantly with the severity of hematologic toxicities ($P > .360$, χ^2 test; Table 1 and Appendix Tables A1 to A3), the levels of haptoglobin were lower in individuals with the Hp 2-2 phenotype than in those with the Hp 2-1 or Hp 1-1 phenotype (Appendix Fig A3, online only).

Construction and Validation of a Model Predicting Hematologic Toxicities

In the M0 cohort (n = 166), 68 patients (41%) experienced category III hematologic toxicities, and 18 patients (11%) experienced category IV hematologic toxicities. Such levels of AE often necessitate the postponement of chemotherapy, and therefore, their prediction before drug administration is desirable. Because none of the parameters, including haptoglobin, was able to predict AEs satisfactorily when used individually (data not shown), we attempted to construct a multivariate predictive model to estimate the relative risk of suffering from hematologic toxicities of category III or worse. We searched for these parameters using a forward stepwise selection procedure by AIC

Information downloaded from jco.ascopubs.org and provided by Kokuritsu Gan Center on March 24, 2009 from .
Copyright © 2009 by the American Society of Clinical Oncology. All rights reserved.

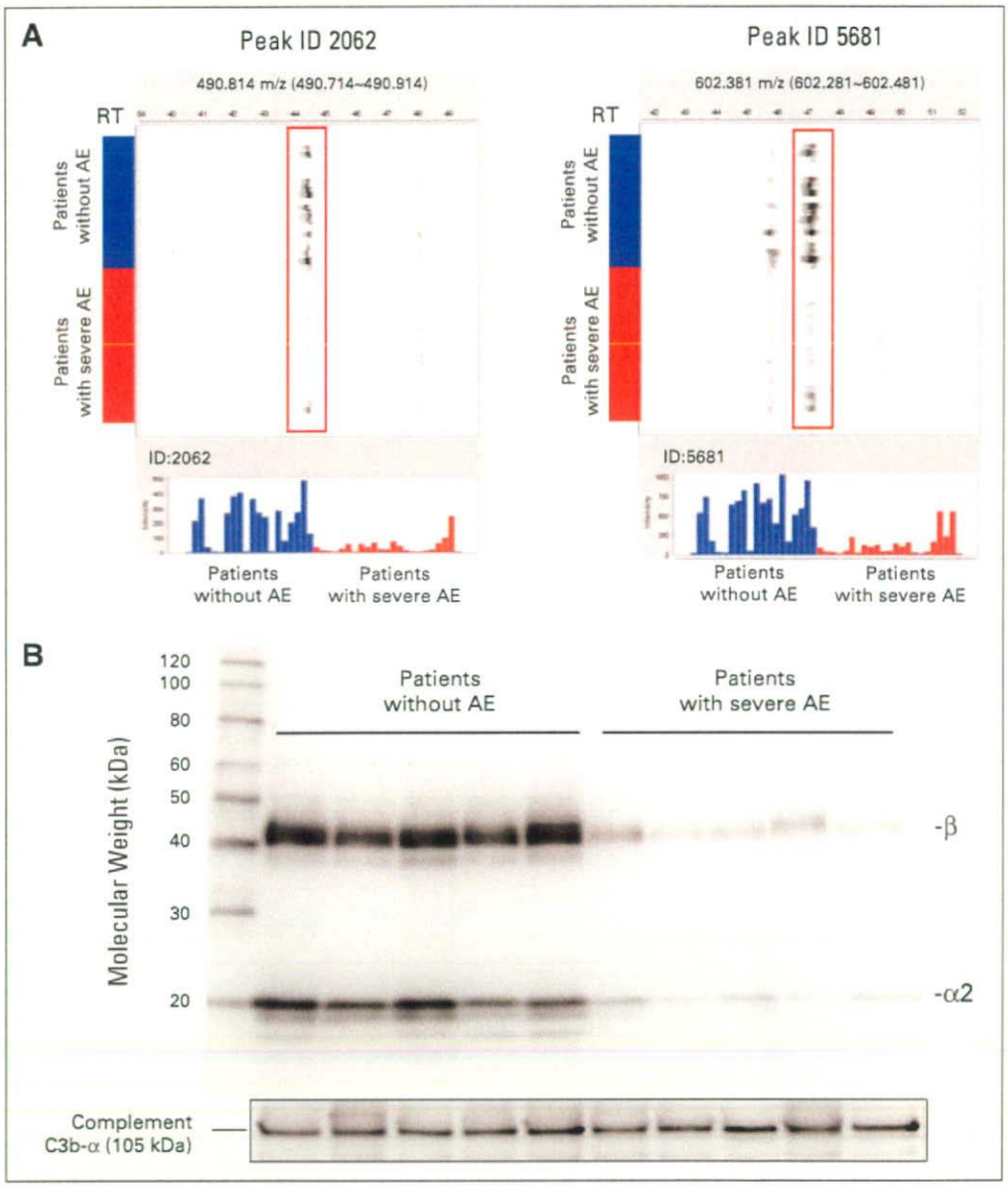

Fig 2. (A) Representative haptoglobin-derived mass spectrometry (MS) peaks in 47 triplicate liquid chromatography (LC)/MS runs (22 without adverse events [AEs], blue; and 25 with severe AEs, red) aligned along the retention time (RT) of LC (top). Columns represent the mean intensity of triplicates (bottom). (B) Detection of β- and α2-chains of haptoglobin and complement C3b-α (loading control) by immunoblotting.

from all of the clinical and laboratory data listed in Appendix Table A1 (available for 162 patients) and found that a combination of plasma haptoglobin level, haptoglobin phenotype, absolute neutrophil count (ANC), platelet count, and body-surface area (BSA) provided the lowest AIC value. The prediction model using this combination of parameters was significantly compromised when haptoglobin level and phenotype were excluded ($\chi^2 = 11.49$, $df = 3$, $P = .009$, likelihood ratio test). We estimated the independent contribution of each parameter to this prediction model and found that the baseline haptoglobin level was the second most important contributor to the model (Table 2).

On the basis of the results of multivariate logistic regression analysis, we constructed a nomogram in which the values of the five parameters (haptoglobin level, haptoglobin phenotype, ANC, platelet count, and BSA) are integrated into a single score (total point) to estimate the relative risk of having hematologic toxicities more severe than category II, category III, or category IV (Fig 4A). The area under the curve value for the prediction of categories III to IV was calculated to be 0.782 (95% CI, 0.711 to 0.843) in cohort M0 (Fig 4B). Predictive ability was confirmed in two independent validation cohorts, V1 and V2, that were not used for construction of the nomogram, with area under the curve values of 0.655 (95% CI, 0.546 to 0.754) and 0.747 (95% CI, 0.606 to 0.858), respectively (Fig 4B).

DISCUSSION

The early onset of severe AE necessitates dose reduction or postponement of treatment, leading to failure of chemotherapy.[30,31] In particular, the current gemcitabine monotherapy against advanced pancreatic cancer is mainly aimed at disease palliation, and thus, avoidance of life-threatening AEs is necessary. In this study, we first compared the plasma proteome of two groups of patients who showed distinct responses to the same protocol of gemcitabine therapy (Fig 1).

© 2009 by American Society of Clinical Oncology

Information downloaded from jco.ascopubs.org and provided by Kokuritsu Gan Center on March 24, 2009 from .
Copyright © 2009 by the American Society of Clinical Oncology. All rights reserved.

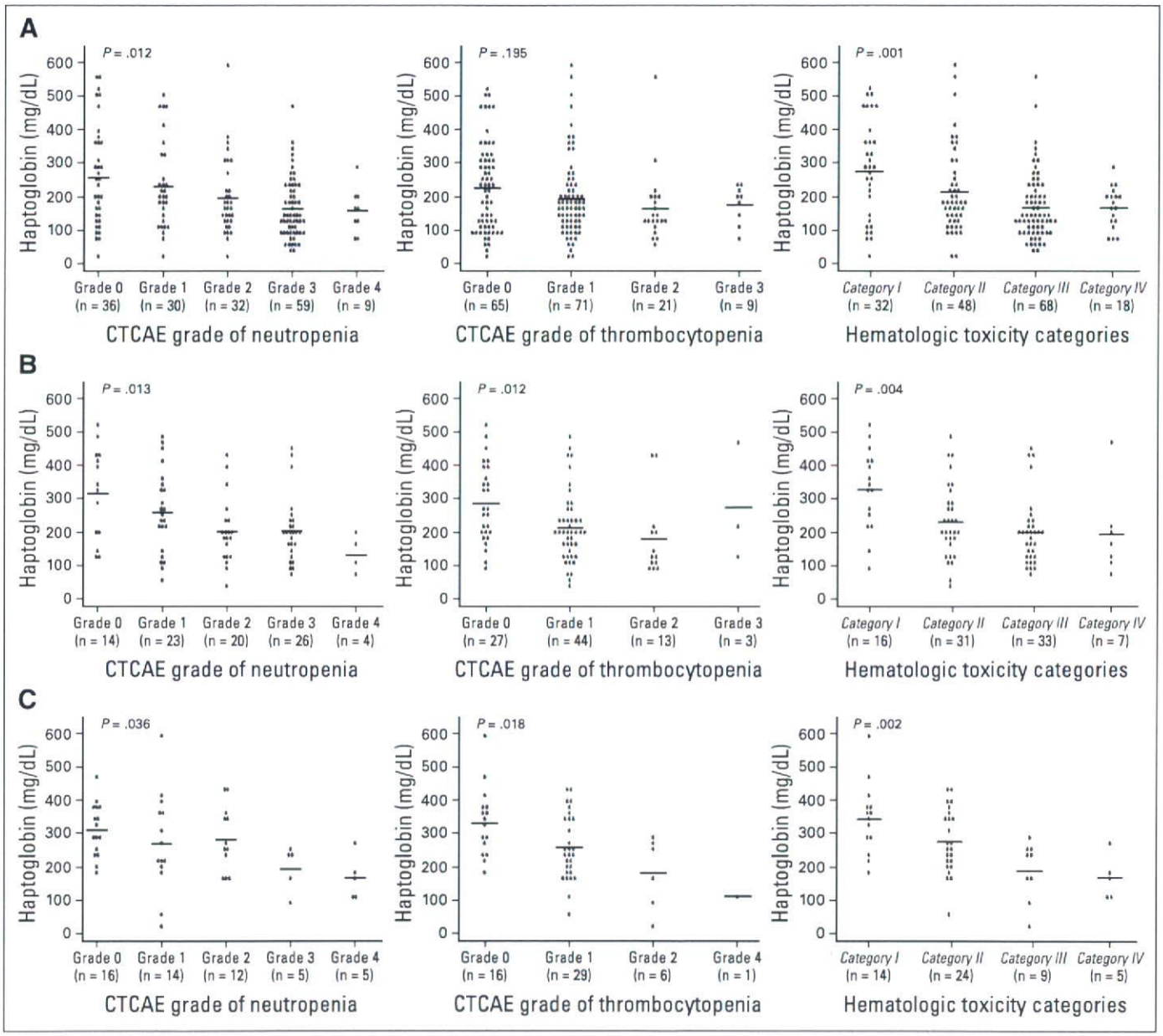

Fig 3. Plasma/serum haptoglobin levels according to the Common Terminology Criteria of Adverse Events (CTCAE; version 3.0). Grades of neutropenia (left), thrombocytopenia (middle), and hematologic toxicity categories (right) in the (A) modeling (M0), (B) validation-1 (V1), and (C) validation-2 (V2) cohorts. Horizontal lines represent the average levels of haptoglobin.

There was no significant difference in age distribution, Eastern Cooperative Oncology Group performance status, liver function, renal function, or prior chemoradiotherapy between the groups (Table 1 and data not shown), indicating that the occurrence of AEs does not merely reflect the general poor condition of patients but is based on certain biologic differences among individuals. We found that individuals who experienced severe AEs after administration of gemcitabine showed decreased baseline levels of plasma haptoglobin (Figs 1B and 2A), and this result was validated in three large cohorts using a different methodology (Fig 3 and Appendix Tables A1 to A3). Haptoglobin is an abundant plasma protein that usually cannot be measured by direct MS. However, constant depletion using an IgY-12 High Capacity Spin Column[32] allowed us to accentuate the differences in haptoglobin levels.

The molecular mechanisms that regulate the plasma haptoglobin level under physiologic and pathologic conditions are largely unknown. Haptoglobin is produced mainly in the liver, taken up by neutrophils, and stored within their cytoplasmic granules. Haptoglobin is released in response to a variety of stimuli, such as infection, trauma, and malignancy,[33] and modulates inflammatory responses. Tumor necrosis factor α induces the release of haptoglobin from neutrophils in vitro.[34] Interestingly, tumor necrosis factor α and its soluble receptors have been reported to be associated with an increased risk of hematologic toxicities.[12,35,36]

 © 2009 by American Society of Clinical Oncology

Information downloaded from jco.ascopubs.org and provided by Kokuritsu Gan Center on March 24, 2009 from .
Copyright © 2009 by the American Society of Clinical Oncology. All rights reserved.

Table 2. Contribution of Parameters to Prediction of Hematologic Toxicities Associated With Gemcitabine

Factor	Odds Ratio*	95% CI	P
Haptoglobin level	0.71	0.53 to 0.97	.031†
Phenotype of haptoglobin (*v* Hp 2-2)			
Hp 2-1	0.61	0.31 to 1.21	.159
Hp 1-1	2.16	0.70 to 6.69	.180
Absolute neutrophil count	0.72	0.61 to 0.86	.0003†
Platelet count	0.63	0.39 to 1.01	.056
Body-surface area	3.86	0.63 to 23.76	.145

NOTE. A forward stepwise selection based on Akaike's Information Criterion was used to select parameters for multivariate analysis.

*Odds ratios are per 100 mg/dL increase for haptoglobin level, per 1,000/μL increase for absolute neutrophil count, per $10 \times 10^4/\mu$L increase for platelet, and per 1.00 m^2 increase for body-surface area.

†$P < .05$.

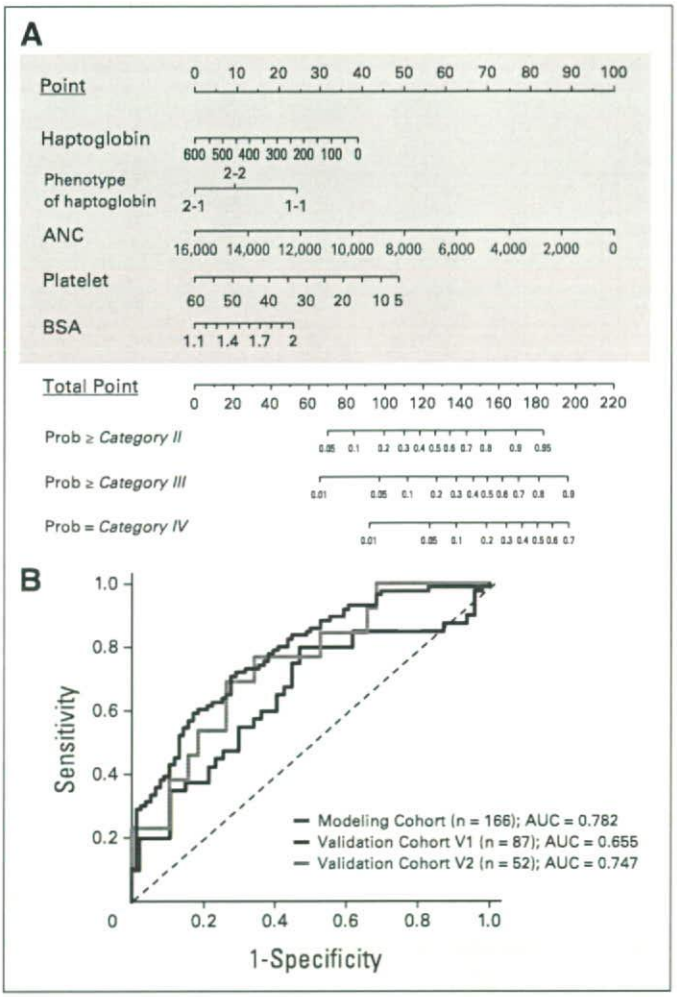

Fig 4. (A) Nomogram to estimate the risk of hematologic toxicities more severe than category II (top), category III (middle), and category IV (bottom). Please see Appendix Figure A4 and its legend for usage. (B) Receiver operating characteristic (ROC) analysis of nomogram for the prediction of category III and IV hematologic toxicities in the modeling (gray), validation-1 (V1; blue), and validation-2 (V2; gold) cohorts. ANC, absolute neutrophil count; BSA, body-surface area; AUC, area under the curve.

To derive clinical applicability from these basic findings, we constructed a model (nomogram) that estimates the possibility of occurrence of hematologic AE before administration of gemcitabine (Fig 4A and Appendix Fig A4). The significance of the model was further confirmed in two independent validation cohorts (Fig 4B). Although its accuracy was far from perfect, the model seems to be practically sufficient for identifying individuals who are likely to suffer from hematologic toxicities after administration of gemcitabine. Various cytotoxic or molecular targeting agents have been tested in combination with gemcitabine in phase III trials, but no apparent additional therapeutic benefit has been demonstrated.[5,6,9,10] The application of this model to patient selection may improve the outcome of such trials. We are now trying to identify new biomarkers that can predict the efficacy of gemcitabine treatment using a similar strategy.

The phenotypes of haptoglobin have been reported to be associated with different hemoglobin-binding, antioxidative, and prostaglandin synthesis–initiating activities.[33] Although haptoglobin phenotype was not significantly associated with hematologic toxicities (Table 1 and Appendix Tables A1 to A3), the average levels of haptoglobin differed among individuals with different phenotypes (Appendix Fig A3), as described previously.[33] For this reason, haptoglobin phenotype was selected in the prediction model by AIC analysis (Table 2). BSA has been repeatedly selected as one of the multivariate parameters for predicting the AEs of anticancer therapies in other studies,[14,37] suggesting a potential lack of accuracy in calculating individually optimized drug dose based solely on BSA, as pointed out previously.[38,39]

In conclusion, we have revealed that a decreased level of haptoglobin is the second most significant factor predicting hematologic toxicities associated with gemcitabine monotherapy after ANC (Table 2). Measurement of haptoglobin is now established as a laboratory test and could be readily incorporated into routine oncologic practice. However, the predictive significance of haptoglobin was revealed only in a retrospective population from a single institution and must, therefore, be validated in an independent prospective multi-institutional study. It was not determined in this study whether haptoglobin could be a predictive biomarker for the AEs of other chemotherapeutic agents. To improve the accuracy of prediction, the discovery of new biomarkers with higher specificity and sensitivity will be necessary. While bearing all these limitations in mind, the present findings may provide novel insights not only into the molecular mechanisms by which gemcitabine causes hematologic toxicities, but also into new avenues for the development of new chemotherapeutic agents with lower toxicity.

AUTHORS' DISCLOSURES OF POTENTIAL CONFLICTS OF INTEREST

Although all authors completed the disclosure declaration, the following author(s) indicated a financial or other interest that is relevant to the subject matter under consideration in this article. Certain relationships marked with a "U" are those for which no compensation was received; those relationships marked with a "C" were compensated. For a detailed description of the disclosure categories, or for more information about ASCO's conflict of interest policy, please refer to the Author Disclosure Declaration and the Disclosures of Potential Conflicts of Interest section in Information for Contributors.

Employment or Leadership Position: None **Consultant or Advisory Role:** None **Stock Ownership:** None **Honoraria:** Nagahiro Saijo, Elli

© 2009 by American Society of Clinical Oncology

Information downloaded from jco.ascopubs.org and provided by Kokuritsu Gan Center on March 24, 2009 from .
Copyright © 2009 by the American Society of Clinical Oncology. All rights reserved.

Lilly **Research Funding:** Nagahiro Saijo, National Institute of Biomedical Innovation **Expert Testimony:** None **Other Remuneration:** None

AUTHOR CONTRIBUTIONS

Conception and design: Junichi Matsubara, Masaya Ono, Setsuo Hirohashi, Tesshi Yamada
Financial support: Nagahiro Saijo, Tesshi Yamada
Administrative support: Tsutomu Chiba, Setsuo Hirohashi
Provision of study materials or patients: Hideki Ueno, Takuji Okusaka, Junji Furuse, Koh Furuta, Emiko Sugiyama, Yoshiro Saito, Nahoko Kaniwa, Junichi Sawada
Collection and assembly of data: Junichi Matsubara, Ayako Negishi, Kazufumi Honda, Nagahiro Saijo, Tesshi Yamada
Data analysis and interpretation: Junichi Matsubara, Masaya Ono, Tomohiro Sakuma
Manuscript writing: Junichi Matsubara, Tesshi Yamada
Final approval of manuscript: Junichi Matsubara, Masaya Ono, Junichi Sawada, Tsutomu Chiba, Nagahiro Saijo, Setsuo Hirohashi, Tesshi Yamada

REFERENCES

1. Honda K, Hayashida Y, Umaki T, et al: Possible detection of pancreatic cancer by plasma protein profiling. Cancer Res 65:10613-10622, 2005
2. Ministry of Health, Labour and Welfare: Japanese Government: Statistical Database 2007. http://wwwdbtk.mhlw.go.jp/toukei/youran/data19k/1-31.xls
3. American Cancer Society: Cancer Facts and Figures 2007. Atlanta, GA: American Cancer Society, 2007
4. Burris HA 3rd, Moore MJ, Andersen J, et al: Improvements in survival and clinical benefit with gemcitabine as first-line therapy for patients with advanced pancreas cancer: A randomized trial. J Clin Oncol 15:2403-2413, 1997
5. Louvet C, Labianca R, Hammel P, et al: Gemcitabine in combination with oxaliplatin compared with gemcitabine alone in locally advanced or metastatic pancreatic cancer: Results of a GERCOR and GISCAD phase III trial. J Clin Oncol 23:3509-3516, 2005
6. Herrmann R, Bodoky G, Ruhstaller T, et al: Gemcitabine plus capecitabine compared with gemcitabine alone in advanced pancreatic cancer: A randomized, multicenter, phase III trial of the Swiss Group for Clinical Cancer Research and the Central European Cooperative Oncology Group. J Clin Oncol 25:2212-2217, 2007
7. National Comprehensive Cancer Network: Clinical Practice Guidelines in Oncology: Pancreatic Adenocarcinoma V. 1. 2008. http://www.nccn.org/professionals/physician_gls/PDF/pancreatic.pdf
8. Casper ES, Green MR, Kelsen DP, et al: Phase II trial of gemcitabine (2,2'-difluorodeoxycytidine) in patients with adenocarcinoma of the pancreas. Invest New Drugs 12:29-34, 1994
9. Kindler HL, Niedzwiecki D, Hollis D, et al: A double-blind, placebo-controlled, randomized phase III trial of gemcitabine (G) plus bevacizumab (B) versus gemcitabine plus placebo (P) in patients (pts) with advanced pancreatic cancer (PC): A preliminary analysis of Cancer and Leukemia Group B (CALGB). J Clin Oncol 25:199s, 2007 (suppl; abstr 4508)
10. Philip PA, Benedetti J, Fenoglio-Preiser C, et al: Phase III study of gemcitabine (G) plus cetuximab versus gemcitabine (C) in patients (pts) with locally advanced or metastatic pancreatic adenocarcinoma (Pca): SWOG S0205 study. J Clin Oncol 25:199s, 2007 (suppl; abstr LBA4509)
11. Ziepert M, Schmits R, Trumper L, et al: Prognostic factors for hematotoxicity of chemotherapy in aggressive non-Hodgkin's lymphoma. Ann Oncol 19:752-762, 2008
12. Voog E, Bienvenu J, Warzocha K, et al: Factors that predict chemotherapy-induced myelosuppression in lymphoma patients: Role of the tumor necrosis factor ligand-receptor system. J Clin Oncol 18:325-331, 2000
13. Pond GR, Siu LL, Moore M, et al: Nomograms to predict serious adverse events in phase II clinical trials of molecularly targeted agents. J Clin Oncol 26:1324-1330, 2008
14. Aslani A, Smith RC, Allen BJ, et al: The predictive value of body protein for chemotherapy-induced toxicity. Cancer 88:796-803, 2000
15. Sugiyama E, Kaniwa N, Kim SR, et al: Pharmacokinetics of gemcitabine in Japanese cancer patients: The impact of a cytidine deaminase polymorphism. J Clin Oncol 25:32-42, 2007
16. Yonemori K, Ueno H, Okusaka T, et al: Severe drug toxicity associated with a single-nucleotide polymorphism of the cytidine deaminase gene in a Japanese cancer patient treated with gemcitabine plus cisplatin. Clin Cancer Res 11:2620-2624, 2005
17. Hanash S: Disease proteomics. Nature 422: 226-232, 2003
18. Yamaguchi U, Nakayama R, Honda K, et al: Distinct gene expression-defined classes of gastrointestinal stromal tumor. J Clin Oncol 26:4100-4108, 2008
19. Taguchi F, Solomon B, Gregorc V, et al: Mass spectrometry to classify non-small-cell lung cancer patients for clinical outcome after treatment with epidermal growth factor receptor tyrosine kinase inhibitors: A multicohort cross-institutional study. J Natl Cancer Inst 99:838-846, 2007
20. Yanagisawa K, Tomida S, Shimada Y, et al: A 25-signal proteomic signature and outcome for patients with resected non-small-cell lung cancer. J Natl Cancer Inst 99:858-867, 2007
21. Ono M, Shitashige M, Honda K, et al: Label-free quantitative proteomics using large peptide data sets generated by nanoflow liquid chromatography and mass spectrometry. Mol Cell Proteomics 5:1338-1347, 2006
22. General Rules for the Study of Pancreatic Cancer (ed 5). Tokyo, Japan Japanese Pancreas Society
23. Honda K, Yamada T, Hayashida Y, et al: Actinin-4 increases cell motility and promotes lymph node metastasis of colorectal cancer. Gastroenterology 128:51-62, 2005
24. Idogawa M, Yamada T, Honda K, et al: Poly(ADP-ribose) polymerase-1 is a component of the oncogenic T-cell factor-4/beta-catenin complex. Gastroenterology 128:1919-1936, 2005
25. Tolson J, Bogumil R, Brunst E, et al: Serum protein profiling by SELDI mass spectrometry: Detection of multiple variants of serum amyloid alpha in renal cancer patients. Lab Invest 84:845-856, 2004
26. Tempero M, Plunkett W, Ruiz Van Haperen V, et al: Randomized phase II comparison of dose-intense gemcitabine: Thirty-minute infusion and fixed dose rate infusion in patients with pancreatic adenocarcinoma. J Clin Oncol 21:3402-3408, 2003
27. Kindler HL, Friberg G, Singh DA, et al: Phase II trial of bevacizumab plus gemcitabine in patients with advanced pancreatic cancer. J Clin Oncol 23: 8033-8040, 2005
28. Cascinu S, Berardi R, Labianca R, et al: Cetuximab plus gemcitabine and cisplatin compared with gemcitabine and cisplatin alone in patients with advanced pancreatic cancer: A randomised, multicentre, phase II trial. Lancet Oncol 9:39-44, 2008
29. Shindo S: Haptoglobin subtyping with anti-haptoglobin alpha chain antibodies. Electrophoresis 11:483-488, 1990
30. Hryniuk W, Bush H: The importance of dose intensity in chemotherapy of metastatic breast cancer. J Clin Oncol 2:1281-1288, 1984
31. Levin L, Hryniuk WM: Dose intensity analysis of chemotherapy regimens in ovarian carcinoma. J Clin Oncol 5:756-767, 1987
32. Huang L, Harvie G, Feitelson JS, et al: Immunoaffinity separation of plasma proteins by IgY microbeads: Meeting the needs of proteomic sample preparation and analysis. Proteomics 5:3314-3328, 2005
33. Langlois MR, Delanghe JR: Biological and clinical significance of haptoglobin polymorphism in humans. Clin Chem 42:1589-1600, 1996
34. Berkova N, Gilbert C, Goupil S, et al: TNF-induced haptoglobin release from human neutrophils: Pivotal role of the TNF p55 receptor. J Immunol 162:6226-6232, 1999
35. Petros WP, Rabinowitz J, Gibbs JP, et al: Effect of plasma TNF-alpha on filgrastim-stimulated hematopoiesis in mice and humans. Pharmacotherapy 18:816-823, 1998
36. Holler E, Kolb HJ, Moller A, et al: Increased serum levels of tumor necrosis factor alpha precede major complications of bone marrow transplantation. Blood 75:1011-1016, 1990
37. Shayne M, Culakova E, Poniewierski MS, et al: Dose intensity and hematologic toxicity in older cancer patients receiving systemic chemotherapy. Cancer 110:1611-1620, 2007
38. Ratain MJ: Body-surface area as a basis for dosing of anticancer agents: Science, myth, or habit? J Clin Oncol 16:2297-2298, 1998
39. Gurney H: Dose calculation of anticancer drugs: A review of the current practice and introduction of an alternative. J Clin Oncol 14:2590-2611, 1996

Acknowledgment

We thank Ayako Igarashi and Yuka Nakamura for their technical assistance.

Information downloaded from jco.ascopubs.org and provided by Kokuritsu Gan Center on March 24, 2009 from .
Copyright © 2009 by the American Society of Clinical Oncology. All rights reserved.

Appendix

Table A1. Clinical and Laboratory Data for Patients in Modeling Cohort (n = 166)

Factor	Neutropenia						Thrombocytopenia					Categorized Hematologic Toxicities				
	Grade 0	Grade 1	Grade 2	Grade 3	Grade 4	*P*	Grade 0	Grade 1	Grade 2	Grade 3	*P*	Category I	Category II	Category III	Category IV	*P*
No. of patients	36	30	32	59	9		65	71	21	9		32	48	68	18	
Haptoglobin, mg/dL						.012					.195					.001
Mean	257	230	196	162	158		225	194	164	174		278	213	166	166	
SD	153	131	116	90	67		132	122	107	56		148	129	99	60	
Haptoglobin phenotype, No. of patients						.599*					.506*					.360*
Hp 2-2	22	18	18	37	3		37	42	11	8		15	30	42	11	
Hp 2-1	11	10	11	18	3		24	20	8	1		14	14	21	4	
Hp 1-1	2	1	2	4	3		3	7	2	0		2	2	5	3	
Sex, No. of patients						.490*					.733*					.797*
Male	21	16	23	40	5		39	45	14	7		18	30	45	12	
Female	15	14	9	19	4		26	26	7	2		14	18	23	6	
Age, years						.719					.418					.912
Mean	63	65	62	63	65		62	64	63	61		63	64	63	63	
SD	7	9	11	9	7		9	9	11	7		9	9	10	7	
ECOG performance status, No. of patients						.674*					.189*					.347*
0	15	14	19	30	7		38	33	12	2		19	21	36	9	
1	19	15	12	26	2		26	33	8	7		13	24	28	9	
2	2	1	1	3	0		1	5	1	0		0	3	4	0	
Body-surface area, m^2						.250					.943					.720
Mean	1.54	1.48	1.55	1.56	1.56		1.55	1.54	1.53	1.52		1.52	1.54	1.56	1.54	
SD	0.19	0.19	0.13	0.17	0.13		0.19	0.14	0.18	0.17		0.21	0.15	0.17	0.15	
Prior therapy, No. of patients						.291					.351					.180
None	31	29	28	47	8		56	62	16	9		28	44	54	17	
CRT using FU for LAPC	5	1	4	12	1		9	9	5	0		4	4	14	1	
Leukocyte, $\times 10^3/\mu L$						< .0001					.019					< .0001
Mean	8.0	6.7	5.4	4.8	4.8		6.5	5.6	5.9	5.3		7.6	6.2	5.2	5.0	
SD	3.5	1.9	1.1	1.5	1.4		2.4	1.9	4.0	1.6		2.6	1.8	2.6	1.5	
Absolute neutrophil count, $\times 10^3/\mu L$						< .0001					.223					< .0001
Mean	6.1	4.8	3.5	3.0	2.6		4.4	3.8	4.1	3.8		5.5	4.4	3.4	3.2	
SD	3.0	1.8	0.9	1.0	0.8		2.1	1.8	3.3	1.4		2.4	1.8	2.1	1.3	
Platelet, $\times 10^4/\mu L$						.198					< .0001					.001
Mean	24	22	21	20	21		25	21	17	16		25	23	20	19	
SD	9	7	6	7	6		7	7	6	7		8	7	7	7	
Hemoglobin, g/dL						.642					.135					.610
Mean	11.9	11.8	12.2	11.8	12.1		12.2	11.7	11.5	11.8		12.0	12.1	11.7	12.0	
SD	1.5	1.3	1.6	1.3	1.6		1.5	1.4	1.4	1.2		1.5	1.6	1.3	1.4	
Albumin, g/dL						.006					.031					.248
Mean	3.5	3.6	3.6	3.7	4.0		3.7	3.6	3.4	3.6		3.7	3.5	3.6	3.8	
SD	0.4	0.5	0.5	0.3	0.3		0.4	0.4	0.5	0.3		0.5	0.5	0.4	0.4	
Creatinine, mg/dL						.697					.621					.485
Mean	0.70	0.65	0.70	0.67	0.71		0.67	0.69	0.67	0.74		0.69	0.67	0.67	0.73	
SD	0.22	0.20	0.23	0.19	0.15		0.20	0.21	0.19	0.21		0.26	0.20	0.19	0.18	
AST, U/L						.084					.148					.071
Mean	38	25	33	37	29		33	32	44	24		34	28	40	26	
SD	25	13	24	23	14		22	20	29	9		24	13	26	12	
ALT, U/L						.051					.298					.044
Mean	44	30	39	46	34		45	37	47	24		44	31	49	29	
SD	36	35	32	40	33		44	31	35	9		43	26	41	24	
ALP, U/L						.109					.300					.648
Mean	693	475	456	457	340		474	479	670	547		537	485	520	444	
SD	619	535	404	327	169		432	418	699	208		525	468	476	212	

NOTE. Kruskal-Wallis test was applied to assess differences of values.

Abbreviations: SD, standard deviation; ECOG, Eastern Cooperative Oncology Group; CRT, chemoradiotherapy; FU, fluorouracil; LAPC, locally advanced pancreatic cancer; ALP, alkaline phosphatase.

*Calculated by χ^2 test.

© 2009 by American Society of Clinical Oncology

Information downloaded from jco.ascopubs.org and provided by Kokuritsu Gan Center on March 24, 2009 from .
Copyright © 2009 by the American Society of Clinical Oncology. All rights reserved.

Table A2. Clinical and Laboratory Data for Patients in Validation Cohort V1 (n = 87)

Factor	Neutropenia						Thrombocytopenia					Categorized Hematologic Toxicities				
	Grade 0	Grade 1	Grade 2	Grade 3	Grade 4	*P*	Grade 0	Grade 1	Grade 2	Grade 3	*P*	Category I	Category II	Category III	Category IV	*P*
No. of patients	14	23	20	26	4		27	44	13	3		16	31	33	7	
Haptoglobin, mg/dL						.013					.012					.004
Mean	317	261	201	204	132		286	213	181	274		327	232	197	193	
SD	138	122	96	97	61		117	106	118	169		123	110	99	131	
Haptoglobin phenotype, No. of patients						.530*					.503*					.804*
Hp 2-2	10	20	13	18	3		20	30	12	2		11	22	26	5	
Hp 2-1	3	3	4	5	1		5	9	1	1		4	6	4	2	
Hp 1-1	1	0	3	3	0		2	5	0	0		1	3	3	0	
Sex, No. of patients						.165*					.307*					.327*
Male	9	14	12	9	1		10	26	7	2		8	20	14	3	
Female	5	9	8	17	3		17	18	6	1		8	11	19	4	
Age, years						.093					.177					.127
Mean	69	62	67	62	71		63	65	68	74		65	65	63	72	
SD	7	10	8	12	10		12	8	10	2		10	8	12	7	
ECOG performance status, No. of patients						.264*					.480*					.038*
0	6	9	11	8	2		13	16	5	2		8	15	9	4	
1	6	12	9	12	2		12	23	6	0		6	16	17	2	
2	2	2	0	6	0		2	5	2	1		2	0	7	1	
Body-surface area, m^2						.425					.982					.427
Mean	1.54	1.57	1.55	1.53	1.41		1.55	1.54	1.54	1.51		1.57	1.55	1.54	1.45	
SD	0.18	0.16	0.17	0.18	0.10		0.17	0.18	0.16	0.17		0.18	0.18	0.16	0.13	
Prior therapy, No. of patients						NA					NA					NA
None	14	23	20	26	4		27	44	13	3		16	31	33	7	
CRT using FU for LAPC	0	0	0	0	0		0	0	0	0		0	0	0	0	
Leukocyte, $\times 10^3/\mu L$						< .0001					.637					.006
Mean	10.4	6.2	5.7	5.8	3.5		7.7	5.7	6.7	6.3		8.9	5.9	6.3	4.7	
SD	7.6	1.4	1.1	3.3	0.5		6.3	1.7	3.1	3.5		7.3	1.3	3.3	2.5	
Absolute neutrophil count, $\times 10^3/\mu L$						< .0001					.807					.013
Mean	7.8	4.2	3.8	3.8	1.7		5.4	3.8	4.6	4.5		6.4	4.0	4.3	2.9	
SD	7.0	1.3	1.0	3.0	0.5		5.9	1.4	2.5	3.0		6.8	1.2	2.9	2.3	
Platelet, $\times 10^4/\mu L$						.062					.001					.001
Mean	25	26	21	22	17		28	21	20	19		31	22	22	18	
SD	6	9	7	6	4		8	6	5	9		9	5	6	6	
Hemoglobin, g/dL						.633					.729					.738
Mean	11.5	12.1	11.9	11.7	11.7		11.6	11.9	12.2	11.0		11.4	12.1	11.8	11.4	
SD	1.1	2.3	1.7	1.5	0.9		1.6	1.6	1.6	3.9		1.9	1.5	1.7	2.4	
Albumin, g/dL						.376					.671					.723
Mean	3.5	3.7	3.6	3.6	3.7		3.6	3.6	3.6	3.3		3.7	3.6	3.6	3.5	
SD	0.4	0.4	0.4	0.4	0.4		0.5	0.4	0.3	0.6		0.4	0.4	0.4	0.5	
Creatinine, mg/dL						.567					.628					.502
Mean	0.66	0.68	0.71	0.68	0.55		0.66	0.69	0.67	0.63		0.68	0.68	0.69	0.59	
SD	0.19	0.21	0.18	0.20	0.06		0.25	0.17	0.15	0.15		0.26	0.18	0.19	0.11	
AST, U/L						.244					.368					.804
Mean	39	38	25	25	20		28	30	34	43		31	32	29	30	
SD	27	31	12	12	4		14	25	26	31		17	27	20	22	
ALT, U/L						.106					.302					.544
Mean	41	44	25	30	15		32	32	41	32		33	35	36	22	
SD	41	49	19	31	2		25	42	40	17		19	46	37	14	
ALP, U/L						.001					.131					.175
Mean	902	546	291	319	187		450	387	693	616		520	440	469	371	
SD	1,003	460	147	223	54		343	454	928	442		374	522	626	345	

NOTE. Kruskal-Wallis test was applied to assess differences of values.

Abbreviations: SD, standard deviation; ECOG, Eastern Cooperative Oncology Group; NA, not applicable; CRT, chemoradiotherapy; FU, fluorouracil; LAPC, locally advanced pancreatic cancer; ALP, alkaline phosphatase.

*Calculated by χ^2 test.

 © 2009 by American Society of Clinical Oncology

Information downloaded from jco.ascopubs.org and provided by Kokuritsu Gan Center on March 24, 2009 from .
Copyright © 2009 by the American Society of Clinical Oncology. All rights reserved.

Table A3. Clinical and Laboratory Data for Patients in Validation Cohort V2 (n = 52)

Factor	Neutropenia						Thrombocytopenia					Categorized Hematologic Toxicities				
	Grade 0	Grade 1	Grade 2	Grade 3	Grade 4	*P*	Grade 0	Grade 1	Grade 2	Grade 4	*P*	Category I	Category II	Category III	Category IV	*P*
No. of patients	16	14	12	5	5		16	29	6	1		14	24	9	5	
Haptoglobin, mg/dL						.036					.018					.002
Mean	310	270	282	194	167		332	256	180	109		343	275	188	167	
SD	81	152	97	70	65		106	98	113	—		109	97	92	65	
Haptoglobin phenotype, No. of patients						.583*					.535*					.621*
Hp 2-2	8	7	4	3	3		6	15	3	1		6	11	5	3	
Hp 2-1	6	6	5	2	2		8	11	2	0		6	10	3	2	
Hp 1-1	2	0	3	0	0		2	3	0	0		2	3	0	0	
Sex, No. of patients						.107*					.701*					.811*
Male	11	5	10	3	4		10	19	3	1		9	14	6	4	
Female	5	9	2	2	1		6	10	3	0		5	10	3	1	
Age, years						.627					.344					.103
Mean	62	65	66	66	61		61	65	68	68		60	66	67	61	
SD	8	6	11	12	11		8	10	8	—		7	9	9	11	
ECOG performance status, No. of patients						.440*					.310*					.194*
0	4	5	5	0	3		2	11	3	1		1	10	3	3	
1	10	6	5	4	1		11	13	2	0		10	10	5	1	
2	2	3	2	1	1		3	5	1	0		3	4	1	1	
Body-surface area, m^2						.023					.529					.256
Mean	1.61	1.44	1.57	1.52	1.67		1.57	1.54	1.53	1.79		1.58	1.52	1.53	1.67	
SD	0.18	0.10	0.17	0.14	0.15		0.19	0.16	0.16	—		0.19	0.16	0.15	0.15	
Prior therapy, No. of patients						NA					NA					NA
None	16	14	12	5	5		16	29	6	1		14	24	9	5	
CRT using FU for LAPC	0	0	0	0	0		0	0	0	0		0	0	0	0	
Leukocyte, $\times 10^3/\mu L$						.006					.649					.146
Mean	8.5	6.3	6.2	5.1	5.0		7.0	6.6	6.7	5.8		7.0	7.1	6.0	5.0	
SD	3.3	1.9	1.5	0.5	1.4		2.1	3.0	1.8	—		2.2	3.1	1.6	1.4	
Absolute neutrophil count, $\times 10^3/\mu L$						.0003					.307					.030
Mean	6.1	4.2	3.8	3.0	2.8		4.6	4.5	4.5	2.4		4.7	4.9	3.9	2.8	
SD	2.7	1.3	1.2	0.4	0.4		1.5	2.5	1.6	—		1.5	2.6	1.5	0.4	
Platelet, $\times 10^4/\mu L$						.562					.0005					.012
Mean	22	22	24	22	19		27	22	16	11		27	22	19	19	
SD	5	8	4	10	5		6	4	5	—		6	4	8	5	
Hemoglobin, g/dL						.087					.703					.240
Mean	12.5	11.8	12.0	13.2	12.0		12.2	12.1	12.5	12.3		12.1	12.1	12.8	12.0	
SD	1.0	1.6	1.4	0.5	0.7		1.4	1.4	0.7	—		1.4	1.5	0.8	0.7	
Albumin, g/dL						.529					.227					.400
Mean	3.7	3.6	3.7	3.7	3.9		3.7	3.6	3.8	4.4		3.7	3.6	3.7	3.9	
SD	0.4	0.3	0.4	0.3	0.4		0.3	0.4	0.3	—		0.4	0.4	0.2	0.4	
Creatinine, mg/dL						.256					.109					.149
Mean	0.71	0.61	0.72	0.72	0.82		0.66	0.69	0.77	1.10		0.66	0.67	0.77	0.82	
SD	0.19	0.14	0.08	0.13	0.27		0.17	0.16	0.10	—		0.18	0.14	0.11	0.27	
AST, U/L						.555					.065					.081
Mean	32	27	41	25	45		23	31	67	63		23	30	52	45	
SD	21	15	46	5	25		9	18	61	—		9	16	53	25	
ALT, U/L						.381					.105					.117
Mean	38	26	54	29	69		26	43	63	33		24	41	49	69	
SD	39	15	56	12	63		17	45	55	—		18	41	49	63	
ALP, U/L						.419					.852					.341
Mean	542	403	400	367	307		446	431	432	259		459	441	437	307	
SD	379	206	178	151	148		334	212	341	—		356	218	279	148	

NOTE. Kruskal-Wallis test was applied to assess differences of values.

Abbreviations: SD, standard deviation; ECOG, Eastern Cooperative Oncology Group; NA, not applicable; CRT, chemoradiotherapy; FU, fluorouracil; LAPC, locally advanced pancreatic cancer; ALP, alkaline phosphatase.

*Calculated by χ^2 test.

© 2009 by American Society of Clinical Oncology

Information downloaded from jco.ascopubs.org and provided by Kokuritsu Gan Center on March 24, 2009 from .
Copyright © 2009 by the American Society of Clinical Oncology. All rights reserved.

Table A4. Plasma Proteins Whose Intensity Significantly Decreased in Patients With Severe Adverse Events

Gene Locus	Accession No.	Identification	Mascot Score	No. of Matched Peptides
HPT_HUMAN	P00738	Haptoglobin precursor	154	6
APOB_HUMAN	P04114	Apolipoprotein B-100 precursor (Apo B-100) (contains: apolipoprotein B-48 [Apo B-48])	89	4
TLN1_HUMAN	Q9Y490	Talin 1	26	3
PLCG2_HUMAN	P16885	1-Phosphatidylinositol-4,5-bisphosphate phosphodiesterase gamma 2 (EC 3.1.4.11)	25	2
HEMO_HUMAN	P02790	Hemopexin precursor (β-1B-glycoprotein)	24	1
CN039_HUMAN	Q8N1H7	Hypothetical protein C14orf39	24	2
RPGF4_HUMAN	Q8WZA2	Rap guanine nucleotide exchange factor 4 (cAMP-regulated guanine nucleotide exchange factor)	20	1
FOXO4_HUMAN	P98177	Putative fork head domain transcription factor AFX1 (Forkhead box protein O4)	18	1
SYNE2_HUMAN	Q8WXH0	Nesprin-2 (nuclear envelope spectrin repeat protein 2) (Syne-2)	18	5
TR240_HUMAN	Q9UHV7	Thyroid hormone receptor-associated protein complex 240 kDa component (Trap240)	17	2
STAB1_HUMAN	Q9NY15	Stabilin-1 precursor (FEEL-1 protein) (MS-1 antigen)	17	2
DEMA_HUMAN	Q08495	Dematin (Erythrocyte membrane protein band 4.9)	17	1
PRS8_HUMAN	P62195	26S protease regulatory subunit 8 (proteasome subunit p45) (p45/SUG) (proteasome 26S subunit)	16	1
PTTG1_HUMAN	O95997	Securin (pituitary tumor-transforming protein 1) (tumor transforming protein 1) (Esp1-associated protein) (hPTTG)	16	1
NCAM2_HUMAN	O15394	Neural cell adhesion molecule 2 precursor (N-CAM 2)	16	1
FNBP3_HUMAN	O75400	Formin-binding protein 3 (Huntingtin yeast partner A) (Huntingtin-interacting protein HYPA/FBP11) (Fas-ligand associated factor 1) (NY-REN-6 antigen)	16	1
RPP38_HUMAN	P78345	Ribonuclease P protein subunit p38 (EC 3.1.26.5) (RNaseP protein p38)	16	1
PRDX1_HUMAN	Q06830	Peroxiredoxin 1 (EC 1.11.1.15) (thioredoxin peroxidase 2) (thioredoxin-dependent peroxide)	15	1
RAI3_HUMAN	Q8NFJ5	Retinoic acid induced 3 protein (G-protein coupled receptor family C group 5 member A) (retinoic acid induced gene 1 protein) (RAIG-1) (orphan G-protein coupling receptor PEIG-1)	15	3
WF10B_HUMAN	Q8IUB3	Protein WFDC10B precursor	15	2
ALU4_HUMAN	P39191	Alu subfamily SB2 sequence contamination warning entry	15	2

Table A5. Plasma Proteins Whose Intensity Significantly Increased in Patients With Severe Adverse Events

Gene Locus	Accession No.	Identification	Mascot Score	No. of Matched Peptides
CERU_HUMAN	P00450	Ceruloplasmin precursor (EC 1.16.3.1) (ferroxidase)	66	1
IC1_HUMAN	P05155	Plasma protease C1 inhibitor precursor (C1 Inh) (C1Inh)	49	1
ITIH2_HUMAN	P19823	Inter-alpha-trypsin inhibitor heavy chain H2 precursor (ITI heavy chain H2)	37	1
KI67_HUMAN	P46013	Antigen KI-67	31	4
LEPR_HUMAN	P48357	Leptin receptor precursor (LEP-R) (OB receptor) (OB-R) (HuB219)	30	3
ATP7B_HUMAN	P35670	Copper-transporting ATPase 2 (EC 3.6.3.4) (copper pump 2) (Wilson disease-associated protein)	30	3
STA13_HUMAN	Q9Y3M8	StAR-related lipid transfer protein 13 (StARD13) (START domain-containing protein 13)	25	2
S23A1_HUMAN	Q9UHI7	Solute carrier family 23, member 1 (sodium dependent vitamin C transporter 1) (hSVCT1)	25	2
KIF23_HUMAN	Q02241	Kinesin-like protein KIF23 (mitotic kinesin-like protein-1) (kinesin-like protein 5)	21	2
CO3A1_HUMAN	P02461	Collagen alpha 1(III) chain precursor	21	2
FRAS1_HUMAN	Q86XX4	Extracellular matrix protein FRAS1 precursor	20	3
ZN236_HUMAN	Q9UL36	Zinc finger protein 236	20	2
PCDH1_HUMAN	Q08174	Protocadherin 1 precursor (protocadherin 42) (PC42) (Cadherin-like protein 1)	20	2
SETX_HUMAN	Q7Z333	Probable helicase senataxin (EC 3.6.1.-) (SEN1 homolog)	20	1
DYH9_HUMAN	Q9NYC9	Ciliary dynein heavy chain 9 (axonemal beta dynein heavy chain 9)	20	2
DYH5_HUMAN	Q8TE73	Ciliary dynein heavy chain 5 (axonemal beta dynein heavy chain 5) (HL1)	19	3
FAS_HUMAN	P49327	Fatty acid synthase (EC 2.3.1.85) [includes: [Acyl-carrier-protein] *S*-acetyltransferase (EC 2.3.1.38); [Acyl-carrier-protein] *S*-malonyltransferase (EC 2.3.1.39); 3-oxoacyl-[acyl-carrier-protein] synthase (EC 2.3.1.41)	19	2
SYSM_HUMAN	Q9NP81	Seryl-tRNA synthetase, mitochondrial precursor (EC 6.1.1.11) (serine--tRNA ligase) (SerRSmt)	19	2
K1949_HUMAN	Q6NYC8	Protein KIAA1949	19	2
KLHL4_HUMAN	Q9C0H6	Kelch-like protein 4	18	3

 © 2009 by American Society of Clinical Oncology

Information downloaded from jco.ascopubs.org and provided by Kokuritsu Gan Center on March 24, 2009 from .
Copyright © 2009 by the American Society of Clinical Oncology. All rights reserved.

CTCAE version 3 .0	Grade 0	Grade 1	Grade 2	Grade 3	Grade 4
Neutropenia	Normal	LLN – 1,500/mm³	1,500 – 1,000/mm³	1,000 – 500/mm³	< 500/mm³
Thrombocytopenia	Normal	LLN – 7.5×10^4/mm³	7.5×10^4 – 5.0×10^4/mm³	5.0×10^4 – 2.5×10^4/mm³	< 2 .5 × 10^4/mm³

Category I *Category II* *Category III* *Category IV*

Fig A1. Category classification of hematologic toxicities based on the worst Common Terminology Criteria of Adverse Events (CTCAE) grades of neutropenia and thrombocytopenia during the first two cycles of gemcitabine monotherapy. LLN, lower limit of normal.

© 2009 by American Society of Clinical Oncology

Information downloaded from jco.ascopubs.org and provided by Kokuritsu Gan Center on March 24, 2009 from .
Copyright © 2009 by the American Society of Clinical Oncology. All rights reserved.

A

Peak ID: 2062

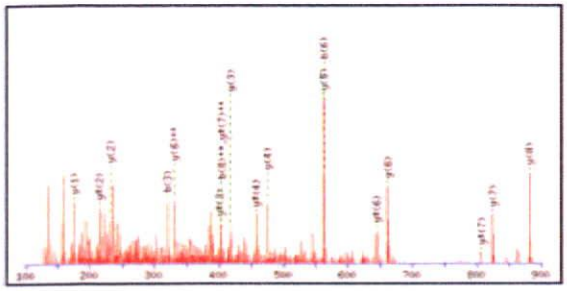

MS/MS Fragmentation of **VGYVSGWGR**
Found in HPT_HUMAN, Haptoglobin precursor
[Contains: Haptoglobin alpha chain; Haptoglobin beta chain] -Homo sapiens (Human)
Match to Query 5: 979.525826 from(490.770189,2+)

Monoisotopic mass of neutral peptide Mr(calc): 979.4876
Ions Score: 47 Expect: 0.0027
Matches (**Bold**): 18/64 fragment ions using 31 most intense peaks

#	a	a++	b	b++	Seq.	y	y++	y*	y*++	#
1	72.0808	36.5440	100.0757	50.5415	V					9
2	129.1022	65.0548	157.0972	79.0522	G	881.4264	441.2169	864.3999	432.7036	8
3	292.1656	146.5864	320.1605	160.5839	Y	824.4050	412.7061	807.3784	404.1928	7
4	391.2340	196.1206	419.2289	210.1181	V	661.3416	331.1745	644.3151	322.6612	6
5	478.2660	239.6366	506.2609	253.6341	S	562.2732	281.6402	545.2467	273.1270	5
6	535.2875	268.1474	563.2824	282.1448	G	475.2412	238.1242	458.2146	229.6110	4
7	721.3668	361.1870	749.3617	375.1845	W	418.2197	209.6135	401.1932	201.1002	3
8	778.3883	389.6978	806.3832	403.6952	G	232.1404	116.5738	215.1139	108.0606	2
9					R	175.1190	88.0631	158.0924	79.5498	1

B

Peak ID: 5681

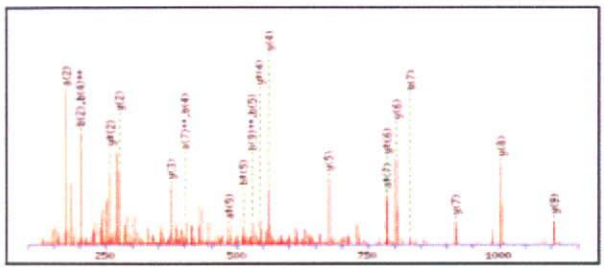

MS/MS Fragmentation of **VTSIQDWVQK**
Found in HPTR_HUMAN, Haptoglobin-related protein precursor -Homo sapiens (Human)
Match to Query 1: 1202.722496 from(602.368524,2+)

Monoisotopic mass of neutral peptide Mr(calc): 1202.6295
Ions Score: 50 Expect: 0.0016
Matches (**Bold**): 22/92 fragment ions using 37 most intense peaks

#	a	a++	a*	a*++	b	b++	b*	b*++	Seq.	y	y++	y*	y*++	#
1	72.0808	36.5440			100.0757	50.5415			V					10
2	173.1285	87.0679			201.1234	101.0653			T	1104.5684	552.7878	1087.5419	544.2746	9
3	260.1605	130.5839			288.1554	144.5813			S	1003.5207	502.2640	986.4942	493.7507	8
4	373.2445	187.1259			401.2395	201.1234			I	916.4887	458.7480	899.4621	450.2347	7
5	501.3031	251.1552	484.2766	242.6419	529.2980	265.1527	512.2715	256.6394	Q	803.4046	402.2060	786.3781	393.6927	6
6	616.3301	308.6687	599.3035	300.1554	644.3250	322.6661	627.2984	314.1529	D	675.3461	338.1767	658.3195	329.6634	5
7	802.4094	401.7083	785.3828	393.1951	830.4043	415.7058	813.3777	407.1925	W	560.3191	280.6632	543.2926	272.1499	4
8	901.4778	451.2425	884.4512	442.7293	929.4727	465.2400	912.4462	456.7267	V	374.2398	187.6235	357.2132	179.1103	3
9	1029.5364	515.2718	1012.5098	506.7585	1057.5313	529.2693	1040.5047	520.7560	Q	275.1714	138.0893	258.1448	129.5761	2
10									K	147.1128	74.0600	130.0863	65.5468	1

Fig A2. Tandem mass spectrometry (MS/MS) spectra and database search results of representative two MS peaks, (A) ID 2062 and (B) ID 5681, identified to be derived from haptoglobin. Peptides that matched the amino acid sequences in the database are highlighted in red.

 © 2009 by American Society of Clinical Oncology

Information downloaded from jco.ascopubs.org and provided by Kokuritsu Gan Center on March 24, 2009 from .
Copyright © 2009 by the American Society of Clinical Oncology. All rights reserved.

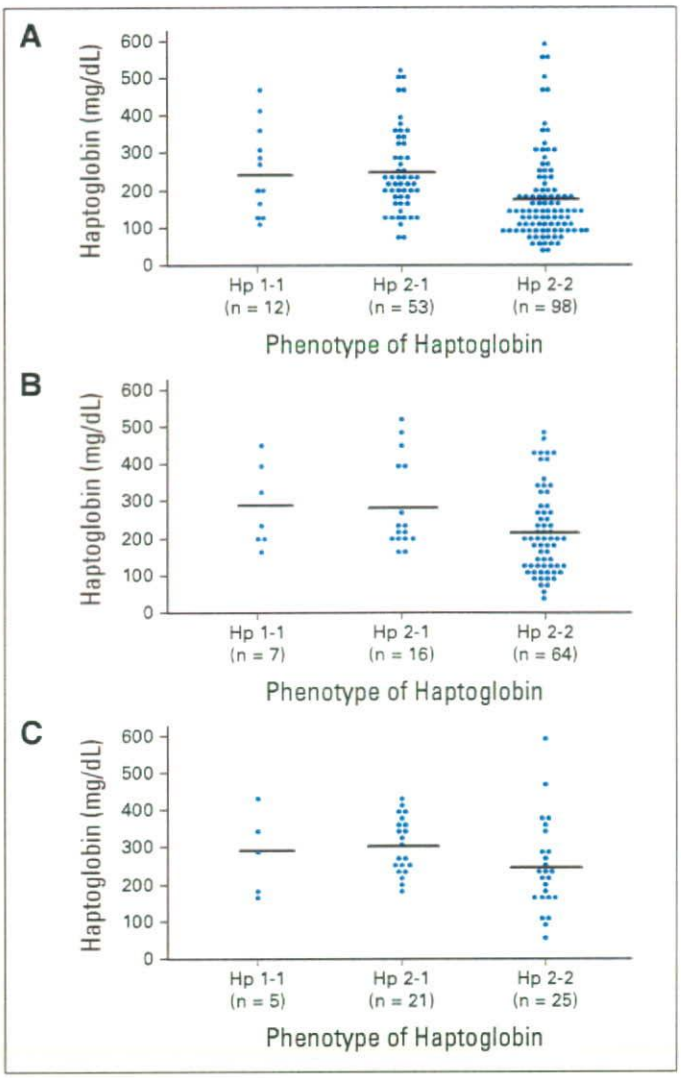

Fig A3. Plasma or serum levels of haptoglobin of individuals with the Hp 1-1 (left), Hp 2-1 (middle), and Hp 2-2 (right) phenotypes. The individuals with the Hp 2-2 phenotype had lower levels of haptoglobin than those with the other phenotypes: (A) modeling cohort, $P < .0001$; (B) validation-1 cohort, $P = .048$; and (C) validation-2 cohort, $P = .068$ (Kruskal-Wallis test).

© 2009 by American Society of Clinical Oncology

Information downloaded from jco.ascopubs.org and provided by Kokuritsu Gan Center on March 24, 2009 from .
Copyright © 2009 by the American Society of Clinical Oncology. All rights reserved.

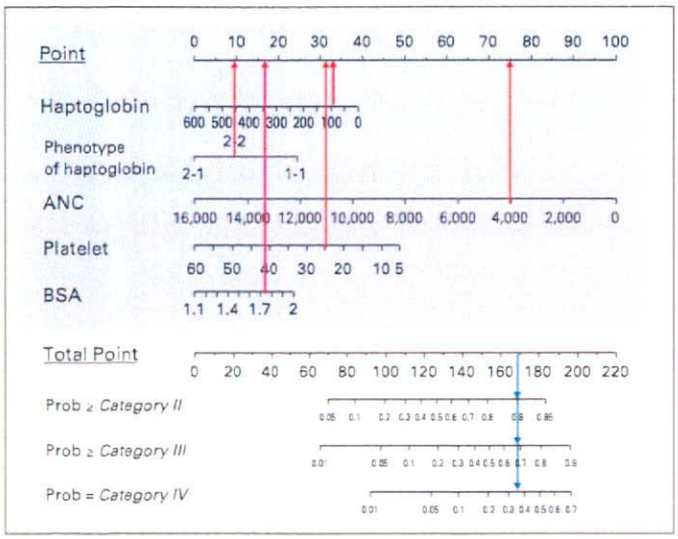

Fig A4. First, draw a vertical line (red) upward to the Point row (top) to obtain the number of points for each variable (top). Then, total the points and drop a vertical line (blue) from the Total Point row to obtain the probability (%) of having hematologic toxicities (bottom). ANC, absolute neutrophil count (/μL); BSA, body-surface area; Prob, probability. If we set a total points cutoff that gave the highest ratio of true-positive plus true-negative patients to all patients in the modeling (M0) cohort, the accuracy for the prediction of categories III to IV in the M0, validation-1 (V1), and validation-2 (V2) cohorts would have been 0.716, 0.609, and 0.725, respectively.

 © 2009 by American Society of Clinical Oncology

Information downloaded from jco.ascopubs.org and provided by Kokuritsu Gan Center on March 24, 2009 from .
Copyright © 2009 by the American Society of Clinical Oncology. All rights reserved.